

Socioeconomic disparities in mobility behavior during the COVID-19 pandemic in developing countries

Lorenzo Lucchini^{1,2,3,4*}, Ollin D. Langle-Chimal^{3,5*}, Lorenzo Candeago³, Lucio Melito³, Alex Chunet³, Aleister Montfort³, Bruno Lepri⁴, Nancy Lozano-Gracia³, Samuel P. Fraiberger^{3,6,7,8}

¹Centre for Social Dynamics and Public Policy, Bocconi University, Milan, Italy.

²Institute for Data Science and Analytics, Bocconi University, Milan, Italy.

³World Bank Group, Washington, DC, USA.

⁴Fondazione Bruno Kessler, Trento, Italy.

⁵University of Vermont, Burlington, VT, USA.

⁶Massachusetts Institute of Technology, Cambridge, MA, USA.

⁷New York University, New York, NY.

⁸To whom correspondence should be addressed.

E-mail: sfraiberger@worldbank.org.

*These authors contributed equally to the work.

Abstract

Mobile phone data have played a key role in quantifying human mobility during the COVID-19 pandemic. Existing studies on mobility patterns have primarily focused on regional aggregates in high-income countries, obfuscating the accentuated impact of the pandemic on the most vulnerable populations. By combining geolocation data from mobile phones and population census for 6 middle-income countries across 3 continents between March and December 2020, we uncovered common disparities in the behavioral response to the pandemic across socioeconomic groups. When the pandemic hit, urban users living in low-wealth neighborhoods were less likely to respond by self-isolating at home, relocating to rural areas, or refraining from commuting to work. The gap in the behavioral responses between socioeconomic groups persisted during the entire observation period. Among low-wealth users, those who used to commute to work in high-wealth neighborhoods pre-pandemic were particularly at risk, facing both the reduction in activity in the high-wealth neighborhood and being more likely to be affected by public transport closures

due to their longer commute distances. While confinement policies were predominantly country-wide, these results suggest a role for place-based policies informed by mobility data to target aid to the most vulnerable.

Keywords: human mobility, mobile phone data, COVID-19, developing countries

1 Introduction

Since its emergence in late 2019, SARS-CoV-2 has led to millions of infections and deaths worldwide, disrupted economies, strained healthcare systems, and caused social and psychological challenges for many individuals and communities at an unprecedented scale. With no vaccine in sight in the early stages of the pandemic, governments and local authorities quickly implemented non-pharmaceutical interventions (NPIs), such as stay-at-home orders or workplace closures, aiming to reduce physical contacts [1–6]. Such measures coupled with the fear of the virus triggered an unimaginable reduction in mobility, which contributed to slowing down the spread of the disease [7–10]. However, these policies were predominantly untargeted, with little regard to socioeconomic status or need, prompting questions on the differentiated impact of the pandemic on the most vulnerable populations [11].

Over the past decade, mobile phone data have become the primary source of real-time disaggregated information on human movements [12–14], and this trend has accelerated during the pandemic [15–18]. Quantifying human mobility in real-time has been key to anticipating the evolution of the virus and the resulting economic shock. Previous works quantifying mobility during the pandemic, from epidemiological surveillance [19, 20] to policy impact evaluation [21], predominantly focused on high-income countries [22]. While some of these studies have shown that the pandemic has had a more pronounced impact on the most vulnerable [23–29], little is known on the socioeconomic disparities in mobility behavior across middle-income economies. Existing studies on mobility in middle-income countries either focused on aggregated trends without taking into account socioeconomic backgrounds [30, 31] or on country-specific case studies [32–34].

Here, we provided a fine-grained analysis of human mobility across 6 middle-income countries, spanning over 3 continents, during the period from March 2020 to December 2020. Using GPS location data from the mobile device applications of 281 million users, we developed a methodology based on spatiotemporal clustering to accurately infer how a user allocated their time between their home, their workplace, and other locations that they visit. By assigning to each user a wealth proxy derived from census data on the administrative unit where they live, we then characterized the propensity of mobile phone users of various socioeconomic groups to self-isolate at home, relocate to a rural area, or commute to work.

We found that the wealth of the neighborhood where a user lives is a strong determinant of their mobility behavior during the pandemic, and our results are remarkably consistent across countries. Relative to the pre-pandemic period, users living in an administrative unit of a metropolitan area where the top 20% richest people are located (“high-wealth place”) were 1.9 times more likely to self-isolate than those living in the bottom 40% (“low-wealth place”), they were 2.9 times more likely to relocate to a rural area once the pandemic hit,

and 1.3 times more likely to stop commuting to work. While users' mobility slowly started to revert toward pre-pandemic levels, the gap in the behavioral response across socioeconomic groups persisted over the entire observation period. Furthermore, by specifically focusing on users living in low-wealth places, we found that those who used to commute to high-wealth places prior to the pandemic stopped commuting 1.4 times more during the observation period than those who used to commute to low-wealth places. Using a dataset of policy actions standardized across countries, we also discovered that the closure of public transportation was associated with a stronger reduction in commuting for low-wealth users who used to commute to high-wealth places, whereas it had no significant impact on those commuting to low-wealth places. As the ability of the poor to work from home is extremely limited in most developing countries and in particular for low-wealth individuals [35, 36], these findings suggest that attention to vulnerable groups is needed when untargeted policies are implemented. Our results also indicate that, when data to identify vulnerable individuals are not available, place-based policies informed by mobile phone data can be a good substitute to target aid to vulnerable groups.

2 Results

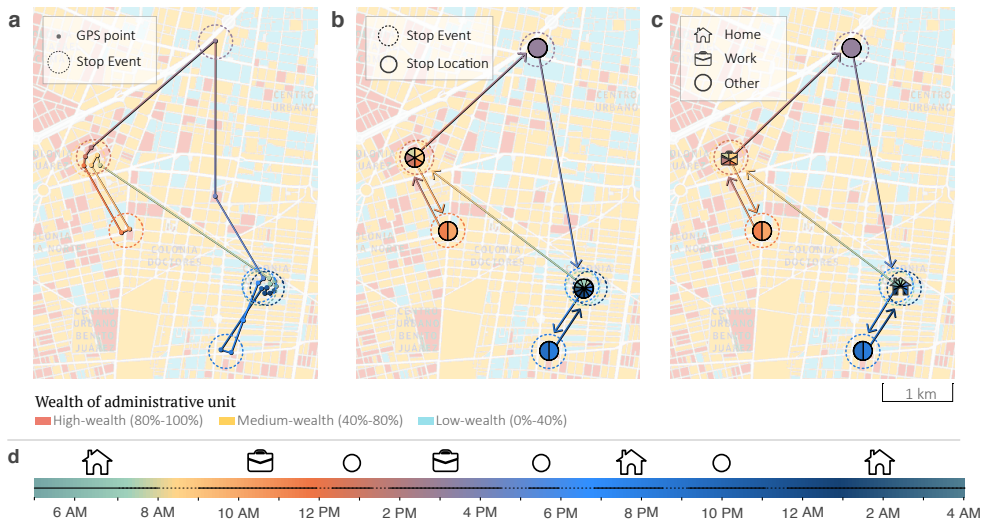


Fig. 1 Inferring location type and time use from GPS trajectories. (a) Trajectory of a hypothetical mobile phone user over the course of one day. A stop event (dotted circle) characterizes a location where a user spends at least 5 minutes within a 25 meter distance. The color of a stop event corresponds to the time of the day when the event occurs, and lines connect two consecutive stop events. (b) Stop events are spatially clustered together to form a stop location. (c) Stop locations are then labeled as *home*, *workplace*, or *other* based on how frequently they are visited during the observation period and the hours of the day at which a visit occurs. (d) Final structure of the user location data, which consists of a non-continuous time-series of labeled stop events. The background image shows a portion of Mexico City where blocks are colored by the level of a wealth index constructed from census data, illustrating the granularity of our data in urban areas.

2.1 Inferring location type and time use

Our GPS dataset comes from Veraset [37] and contains the anonymized timestamped geocoordinates of 281 million mobile phone users located in 6 middle-income countries –Brazil, Colombia, Indonesia, Mexico, Philippines, and South Africa– between January 1st and December 31st, 2020 (“observation period”). We discarded occasional users to focus on the longitudinal behavior of 1.35% of users active on at least 20% of days during the observation period and at least 20% of days between January 1st and March 15th (“pre-pandemic period”). To uncover how users spent their time, we first applied a spatiotemporal clustering algorithm to convert their GPS coordinates into a sequence of stop events where a user spent at least 5 minutes within a 25 meter distance (Figure 1). We then spatially clustered stop events to identify unique locations repeatedly visited by a user over time (“stop locations”). Finally, we classified stop locations as *home*, *workplace*, or *other* based on how frequently they were visited during the observation period and the hours of the day at which a visit occurred. A manually annotated sample of 500 users’ trajectories enabled us to obtain optimal parameter values for our classifier of location type, which reached an out-of-sample classification accuracy of 80% (see Sec. SI 5). Taken together, these steps allowed us to convert a mobile user trajectory into a non-continuous time series of stop events labeled by location type.

2.2 Classifying users by wealth

In the absence of socioeconomic data on individual users, we used the most recent population census in each country to generate a proxy of their wealth from that of the administrative unit where they live [38]. We estimated a one-dimensional wealth index from data on asset ownership and access to services for the most disaggregated level of administrative units in each country (see Materials and Methods). We then assigned to each user the wealth index of the administrative unit where their most frequently visited home during the pre-pandemic period was located (“primary home”). This procedure allowed us to quantify how users who differ by the wealth of their primary home’s administrative unit allocated their time between their homes, their workplaces, and other locations over time. In what follows, we restricted our analysis to the 46% of frequent users whose primary home is located in one of the five most populated cities of each country, where mobile phone users are concentrated. (see Tab. 1 in Material and Methods).

2.3 Self-isolating at home

To characterize mobility behavior during the pandemic, we started by focusing on the propensity of users to self-isolate at home relative to the pre-pandemic period (Fig. 2). In the early stages of the pandemic when no vaccines were available, home self-isolation was the most efficient way to avoid getting infected. We found that, on average, the proportion of high-wealth users self-isolating at home increased about 78% more than that of low-wealth users – 252% versus 141%. The gap between high- and low-wealth groups’ propensity to self-isolate is observed across all 6 countries in our sample, ranging from a difference of 36% for the Philippines to 175% for South Africa. While 55% of users kept spending some of their time outside of home, time spent at home increased on average by 19% for the high-wealth group versus 13% for the low-wealth group. The reduction in time spent outside of home was primarily driven by a reduction in time spent at work, which dropped by 40% on average for the

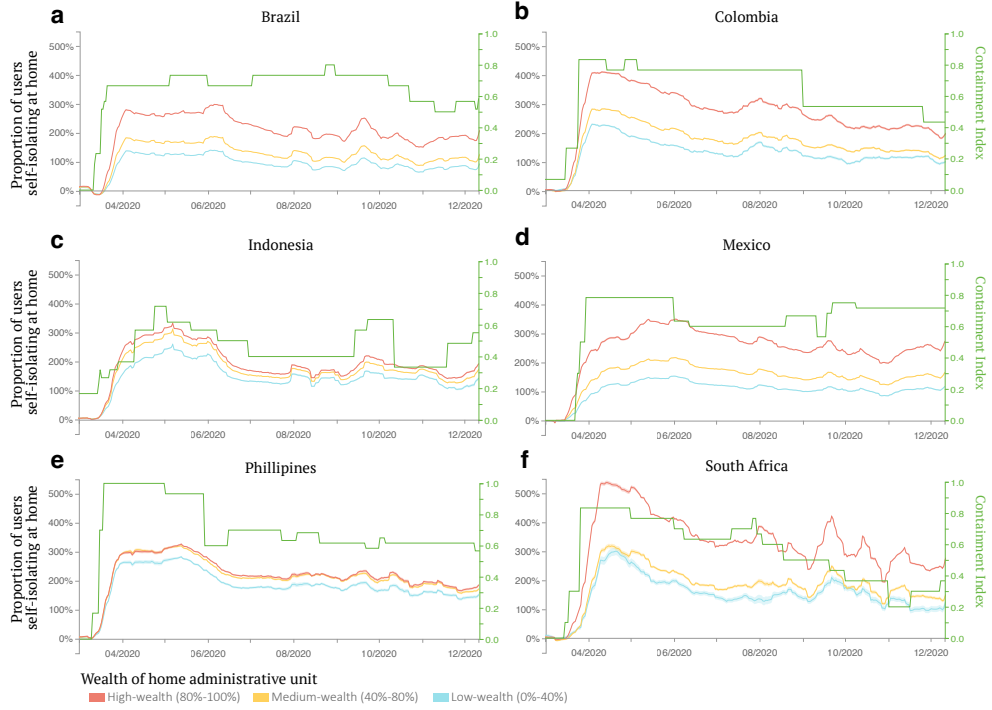


Fig. 2 *Change in the proportion of users self-isolating at home by socioeconomic group.* Each panel shows the relative change in the proportion of active users staying at home over the entire course of a day relative to the pre-pandemic period for the six countries studied, conditioning on the wealth of their primary home administrative unit. Shaded areas indicate standard errors. We also report the stringency index of containment policies in each country over time (green line). Across all countries, users living in high-wealth places were more likely to isolate at home when the pandemic hit than those living in low-wealth places, and the gap persisted during the observation period.

high-wealth group while only 29% for the low-wealth one after the pandemic declaration (Fig. SI 3), suggesting that the capacity to work from home was the main determining factor in the decision to self-isolate. Although the mobility of all socioeconomic groups gradually started to revert back to its pre-pandemic level, the gap between high- and low-wealth groups persisted, indicating that low-wealth groups remained more exposed to physical contact during the observation period.

2.4 Relocating to rural areas

Quantifying population movements between urban and rural areas is key to uncovering how the virus propagated geographically within countries and provides some insights into the capacity of mobile users to respond to the evolution of the pandemic and mobility restrictions. Thanks to our dynamic classification of home locations, we could identify users relocating during the observation period (Fig. 3). Across all 30 cities in our sample, we find that a net flow of about 0.61% of users relocated to rural areas during the first 3 months of the pandemic. Users in the high-wealth group were on average 159% more likely to relocate compared to

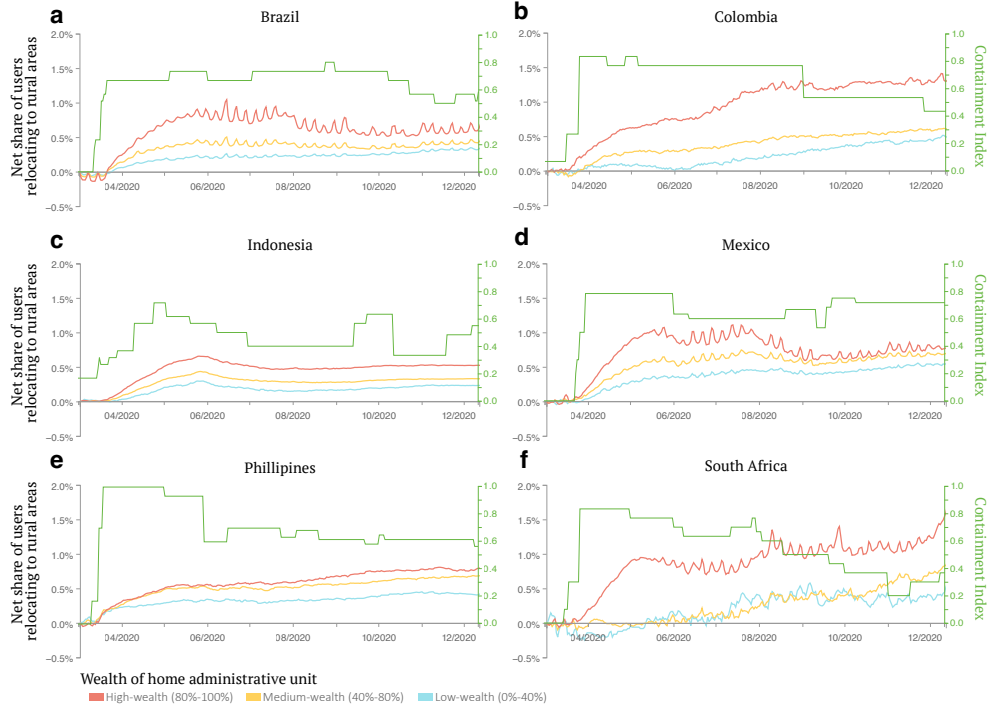


Fig. 3 *Net proportion of urban users relocating to rural areas by socioeconomic group.* Each panel shows the percentage change in the difference between the number of individuals relocating from an urban to a rural area and those moving from rural to urban, for different socioeconomic groups in the six countries under study. Results are normalized to remove pre-pandemic relocation flows. Across all countries, users whose primary home is located in a high-wealth neighborhood (red line) were more likely to relocate to a rural area than those living in a low-wealth neighborhood (blue line).

those in the low-wealth groups, with these average gaps ranging from a 79% difference for the Philippines to a 355% difference for South Africa which faced the largest relocation gap between socioeconomic groups. Relocation flows then remained relatively flat in the latter half of 2020. These patterns are consistent with the more risk-averse users living in high-wealth administrative units having more options than low-wealth users to relocate to less densely populated rural areas to minimize physical contact. Similar results were obtained in high-income countries [39], highlighting the potential acceleration of the virus propagation caused by high-wealth individuals having relocated to rural areas.

2.5 Commuting patterns

A key challenge of untargeted confinement policies stems from the uneven ability to work from home across socioeconomic groups. While this issue has extensively been documented in high-income countries, it is exacerbated in developing countries where only a small fraction of rich individuals can work remotely due to the structure of labor markets, higher levels

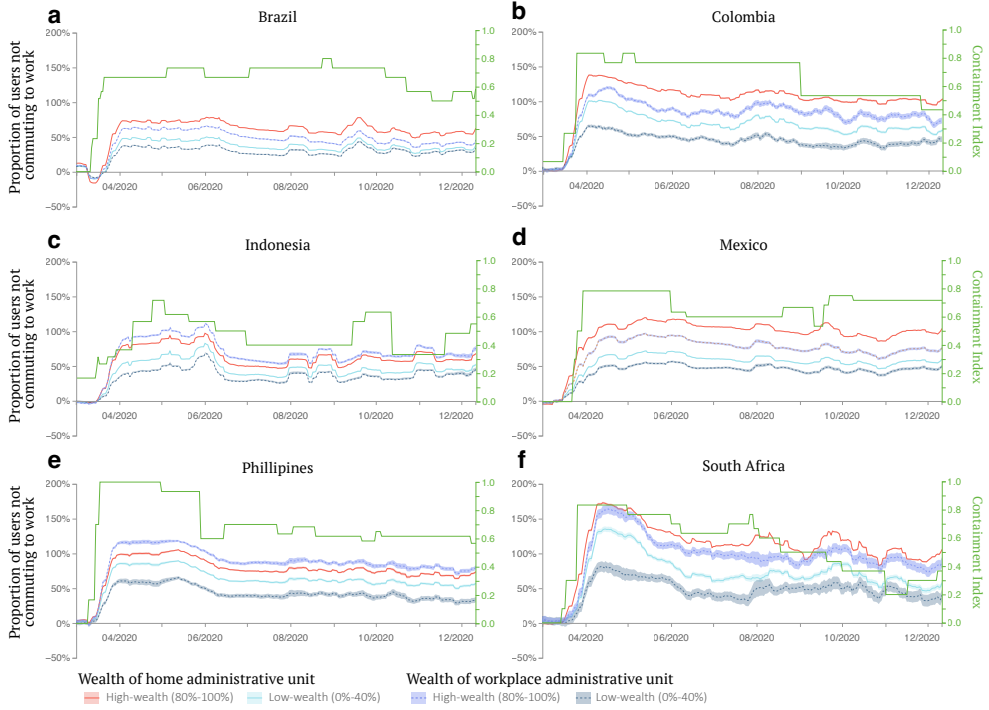


Fig. 4 *Change in the fraction of users not commuting by socioeconomic group.* Focusing on the 26% users with a work location during the observation period, we illustrate the percentage change in the number of individuals who are not commuting, conditioning on their wealth group classification. Users in the high-wealth group (solid orange line) were more likely to stop commuting than those in the low-wealth group (solid blue line). Shaded areas highlight the 2-standard error region. We then restrict to individuals from the low-wealth group and measure their changes in commuting patterns conditioning on the wealth of their workplace. Users living in low-wealth neighborhoods who used to work in high-wealth neighborhoods pre-pandemic (dashed orange line) were more likely to stop commuting than those who used to work in low-wealth neighborhoods (dashed blue line). The shaded region highlights the 2-standard error area. The green line shows the stringency of containment policies in the corresponding countries over time.

of informal employment, reduced internet access, and a lack of compensatory income support [35]. To shed light on these issues, we estimate users' propensity to commute relative to the pre-pandemic period (Fig. 4). Although we do not have fine-grained measures of changes in unemployment, we hypothesize that low-wealth users lack the ability to work from home, and therefore a change in commuting behavior is a good proxy for a change in employment status for this group. We find that the proportion of users who stopped commuting increased sharply in all countries in the early stage of the pandemic. It then reverted before stabilizing in the latter half of 2020. Consistent with our findings on self-isolating behavior, users in the high-wealth group were 52% times more likely to stop commuting compared to users in the low-wealth group once the pandemic started. The difference between high- and low-wealth groups ranges from 23% for the Philippines to 74% for Mexico. We then separated low-wealth users by the wealth of the administrative unit where they used to commute during the

pre-pandemic period. Those who used to commute to high-wealth neighborhoods were about 89% more likely to stop commuting than those who used to commute to low-wealth neighborhoods. These results are consistent with existing studies of high-income countries [40, 41]: high-wealth users' decision to self-isolate led to a reduction in demand for goods and services in high-wealth neighborhoods where they live. This, in turn, predominantly impacted the employment prospects of low-wealth users who used to work in high-wealth neighborhoods before the pandemic started.

2.6 Policy restrictions and mobility behavior

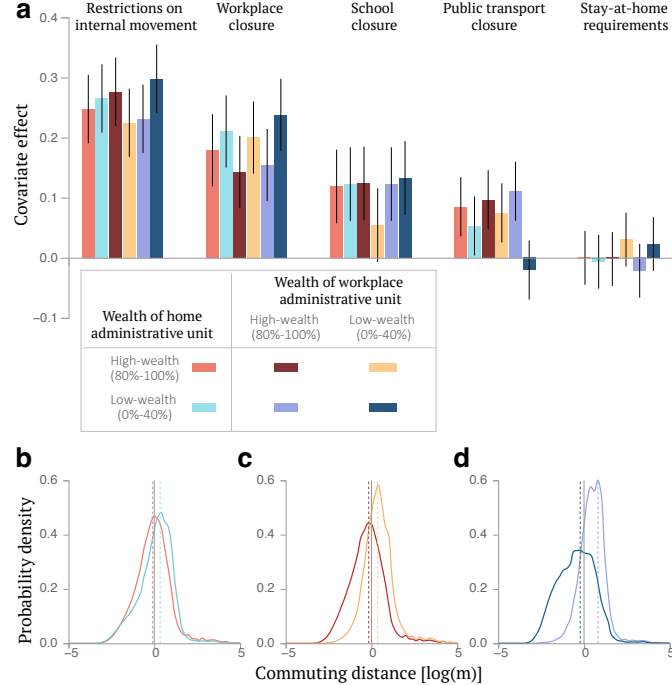


Fig. 5 Policy restrictions and commuting patterns across socioeconomic groups. a) We present the covariate effects of policy restrictions on the propensity of users from different socioeconomic groups to suspend commuting. b-d) Distributions of the distance between home and workplace across socioeconomic groups, b) comparing users living in low- versus high-wealth neighborhoods, then c) focusing on users living in high-wealth neighborhoods and comparing those working in low- versus high-wealth neighborhoods, and d) focusing on users living in low-wealth neighborhoods and comparing those working in low- versus high-wealth neighborhoods.

Taken together, our results indicate that users' mobility changed sharply during the first weeks of the pandemic, predominantly for users located in high-wealth neighborhoods, generating a socioeconomic gap that persisted during the entire observation period. These findings call into question the extent to which government interventions imposing restrictions on mobility to reduce the spread of infections contributed to this gap. We, therefore, analyzed the statistical associations between containment measures –restrictions on internal movement,

school closure, workplace closure, public transport closure, and stay-at-home requirements—and mobility. We specifically focused on the fraction of users commuting to work across wealth groups, an outcome of utmost importance to characterize the distributional impact of containment policies on jobs in a timely fashion. We estimated a multivariate panel regression model for each wealth group, which includes local and global incidence of cases obtained from Our World in Data [42], and stringency indices of policy restrictions from the Oxford COVID-19 Government Response Tracker [43]. All the explanatory variables are independently standardized for each wealth group, therefore our panel regression with fixed effects can be used to elicit relative differences between group-specific responses to containment measures (see Materials and Methods).

The majority of policy restrictions during the observation period were implemented country-wide within a short time frame in the first weeks of the pandemic when people's risk perception of the virus also shifted abruptly (Fig. SI 27). It is therefore difficult to tease out the effect of a single policy enactment happening during this period. To overcome this issue, we estimated our model from April 11, 2020 –one month after the pandemic declaration– to December 31, 2020 (see Sec. SI 10B for additional results over the entire pandemic period). Except for stay-at-home requirements, we found that all containment policies were associated with a higher fraction of users who stopped commuting to work (Fig 5a). As we excluded the first month of the pandemic from the analysis, we did not find a significant difference in mobility response between high- and low-wealth users. However, by focusing specifically on low-wealth users, we found that public transport closures were associated with a significant reduction in commuting for users commuting to high-wealth neighborhoods (coefficient=0.10, 95% confidence interval= [0.05, 0.15]). By contrast, low-wealth users commuting to low-wealth neighborhoods were not significantly affected by such measures. These findings reflect the fact that low-wealth users working in high-wealth neighborhoods are those commuting the longest distances on average, therefore often relying on public transport to get to work, while those working in low-wealth neighborhoods have the shortest commuting distances (Fig. 5b-d). Without conditioning by the wealth of workplace neighborhood, average commuting distances are not statistically different between wealth groups based on their home location, stressing the value of having detailed information on individual users to characterize their behavior.

3 Discussion

GPS data from personal mobile devices have played a key role in providing timely information to quantify the impact of the COVID-19 pandemic. Here, we focused on four upper-middle income countries [22] –Brazil, Colombia, Mexico, and South Africa– and two lower-middle income countries –Indonesia and Philippines– from Latin America, Sub-Saharan Africa, and South East Asia to elicit common disparities across socioeconomic groups in the behavioral responses to the pandemic and containment measures. By analyzing longitudinal data over one year, we quantified the behavior of mobile users living in urban areas in terms of their propensity to self-isolate at home, relocate to rural areas, and suspend their daily commute.

We uncovered a consistent socioeconomic gap in the percentage of users who adapted their mobility behavior in response to the pandemic. Individuals from high-wealth socioeconomic groups were more likely to self-isolate at home and to relocate to rural areas to reduce their exposure to the virus. A greater percentage of high-wealth users stopped their daily commute, reflecting their higher propensity to work from home. On average, we observed wider gaps between high and low-wealth groups in upper-middle-income countries, indicating a greater ability of high-wealth users in these countries to work from home than for lower-middle-income countries [35].

When we focused specifically on the commuting patterns of low-wealth users –who, to a higher degree, lack the ability to work from home– we discovered that in all six countries, those commuting to high-wealth neighborhoods pre-pandemic were more likely to stop commuting during the pandemic than those commuting to low-wealth neighborhoods. By limiting their outside activities or abandoning urban areas, high-wealth individuals amplified the economic shock affecting low-wealth individuals working in high-wealth neighborhoods. Furthermore, owing to their longer commuting distances, low-wealth users working in high-wealth neighborhoods were also more likely to stop commuting following public transport closures, whereas the commuting behavior of those working in low-wealth neighborhoods was not significantly affected by this policy restriction. Taken together, these results indicate that individuals living in low-wealth neighborhoods and working in high-wealth neighborhoods were disproportionately burdened in their ability to work.

These results illustrate the delicate balance between ensuring a forceful response to a pandemic and the unintended consequences resulting from untargeted interventions, which could disproportionately impact economically vulnerable groups. While targeting based on individual information is always preferred, information may not be available or it may be difficult to acquire in cases of emergency where time is of the essence. In such cases, place-based policy interventions may provide an alternative for effective targeting and optimally distributing additional support to the most vulnerable. As developing countries often lack the possibility to access up-to-date information on individuals [44], mobile data could provide a tool to implement such targeted policies in a timely fashion and respond to future pandemics more appropriately.

4 Materials and Methods

4.1 Datasets

Population census

We collected data from the most recent population census in each country to construct a wealth index measuring the socioeconomic level of an administrative unit. We used data on the level of education, access to health services, assets' ownership, and various household and social characteristics for the smallest administrative unit available. These different dimensions are then aggregated into a single index using principal component analysis to produce a one-dimensional wealth index of an administrative unit [45, 46].

Administrative boundaries

Administrative boundaries consist of geolocalized polygons with unique identifiers. They were retrieved from the National Institute of Statistics or the National Institute of Geography website for each country. The spatial-resolution level varies depending on the country. All the administrative boundary files share at least four common administrative levels: national, regional, urban, and suburban units. Administrative boundaries were used to compute the wealth index and mobility patterns across socioeconomic groups.

Urban extents

Urban extents were obtained from the GHS Urban Centre Database (GHS-UCDB). It characterizes spatial entities called “urban centers” according to a set of multitemporal thematic attributes gathered from the Global Human Settlement Layer sources and integrated with other sources available in the open scientific domain. The urban centers are defined by specific cut-off values on resident population and built-up surface share in a 1x1 km uniform global grid. As such, urban extents are defined as contiguous cells (without diagonals and with gap filling) with a density of at least 1,500 inhabitants/km² and a minimum of 50,000 inhabitants. This dataset has global coverage and is therefore well-suited for multi-country applications.

Veraset movements

Mobile data were provided by the data company *Veraset*. It consists of the anonymized timestamped GPS coordinates of mobile devices, covering about 5% of the global population. Their data is sourced from thousands of Software Development Kits (SDKs), which reduces sampling biases [37].

4.2 Mobility data processing

We present a brief description of the procedure to infer relevant information about individual users. We refer to a single GPS point within an individual’s trajectory as “ping”. Each ping has an associated accuracy measure providing an estimate of the coordinates’ precision. Starting from a collection of trajectories we perform a series of steps to identify the types of locations being visited by a user [6]:

1. First, we aggregate pings into stop events, which are clusters of spatiotemporally contiguous pings (for more details, see Sec. SI 3A).
2. Second, we perform an additional spatial clustering step to aggregate stop events that are close enough to be associated with a single location.
3. Third, to reliably assign an individual home location, and to subsequently connect its demographic information, we follow a consolidated approach, which makes use of different heuristics based on circadian rhythms and weekdays-weekend patterns [13, 47–51] (see Sec. SI 3C for details).
4. Fourth, we restrict the set of users to those who appear in our records at least once per day for at least 20% of the days pre-pandemic, and 20% of the days during the observation period (see Sec. SI 3B for additional details).

After these processing steps, we associated each user with a wealth proxy based on the administrative unit where their primary home location is located (Tab. 1). To precisely connect

mobility with demographic data at the smallest sub-urban scale available, further processing is required, which we describe in Sec. SI 4.

	BR	CO	ID	MX	PH	ZA
Active users	1514679	142933	1205827	676775	104681	144445
GPS points	3.9e10	2.9e9	1.9e10	1.7e10	1.9e9	3.4e9
Stop events	1452M	103M	893M	656M	75M	154M
Stop locations	111M	8M	76M	50M	5M	12M
Population fraction	1.7%	0.5%	1.0%	1.6%	0.2%	0.7%
Median area [km²]	0.067	0.003	2.352	0.005	0.483	1.191

Table 1 Summary statistics of the dataset. All the numbers are for active users living in urban administrative units. Population fractions were computed using census data from each country.

Reweighting and wealth labels

GPS data, sourced from mobile phones, are known to potentially introduce biases due to an uneven distribution of wealth among the devices' owners [52, 53]. These biases need to be taken into account in the process of assigning labels to individuals and aggregating them into groups. In general, official demographic data are associated with single individuals based on the smallest sub-urban areas available for each country. While demographic data from the National Institutes of Statistics of each country (see Sec. 4.1) can be considered as an unbiased information source, the process with which we link them with individual GPS information and aggregate them in groups afterward could drastically impact the reliability of the analyses. A simplistic approach would be to group individuals with lower wealth values, based on the wealth of the administrative unit their home location falls in. This would create groups based on mobile-phone user percentiles of wealth. In this framework, given a sample of 100 users, the 40 users with lower wealth would be labeled as “low-wealth individuals”. However, this would automatically transfer biases within the user base into biased wealth groups. Our population-based reweighting approach, in contrast, consists of a top-down classification of wealth groups. Administrative units with which at least one user is associated are considered and divided into wealth categories based both on their average wealth and on the fraction of the population living there. High-wealth, Medium-wealth, and Low-wealth labels are then associated with each administrative unit considering discrete percentile groups. Thus, “low-wealth individuals” will only be represented by those users living in administrative units whose wealth is in the lower 40% of the population wealth (and not the user wealth). We stress that we consider as a population the total number of residents living in all retained administrative units as provided by the most recent demographic data before the pandemic was declared. Table 2 reports the percentages of mobile-phone users in our dataset divided into the three wealth groups that were considered in this analysis. More precisely, high-wealth individuals represent the wealthiest 20% of the population and account, on average, for more than 45% of the user base. In contrast, low-wealth individuals represent the less-wealthy 40% of the population and only accounts for 18% of the mobile-phone user base on average.

	BR	CO	MX	ID	PH	ZA
High wealth	42.17 %	36.75 %	39.85 %	36.58 %	39.48 %	76.77 %
Medium wealth	34.75 %	41.51 %	38.87 %	44.95 %	39.91 %	18.3 %
Low wealth	23.08 %	21.74 %	21.27 %	18.46 %	20.61 %	4.93 %

Table 2 Device distribution per wealth of home location neighborhood. For each country, the percentage of devices labeled within each different group is reported. A biased distribution is found, with high-wealth individuals being more represented than low-wealth individuals.

Commute distances

To compute distances between home and work locations in Fig. 5, we process individual-level information. We take the logarithm of distances to regularize the distribution. Then, log distances are standardized by subtracting the average of all users in a wealth group and dividing by the standard deviation, such that all distributions are centered around 0 with a width of 1.

4.3 Panel regression model

We model the association between mobility indicators and policy restrictions for different socioeconomic groups. Mobility indicators by socioeconomic group are determined by the socioeconomic status of the home and work location of a user. In this framework, the standardized mobility mb_{ic} of group i in country c is modelled as:

$$mb_{ic} = a_i * incidence_g + b_i * incidence_c + \sum_n c_i(n) * C_c(n);$$

where a_i is a cross-country free parameter capturing the group-specific association with the global incidence of COVID-19 reported cases ($incidence_g$), b_i is the cross-country free parameter, pooled over all countries in our panel, to capture the association of the dependant variable with the local incidence of cases ($incidence_c$), and $c_i(n)$ are coefficients modeling the $C(n)$ policy effect on mobility for the i -group. Five different policy types are included in the model discussed in Sec. 2.6: school closure policies, workplace closure policies, public transport closures, internal movement restrictions, and stay-at-home orders. $C(n)$ is the index associated with the n policy and $c_i(n)$ is the corresponding group association coefficient. The choice of the components to include in the model is based on the hierarchical selection of the most important components in a modeling framework where policies are grouped in summary indices (containment, economic, and health) [43]. Model selection is performed using the Bayesian Information Criterion (BIC) comparing models with different covariate compositions. Selection robustness tests, performed on single countries as well as on single wealth-groups BIC values, provide consistent results in terms of model selection. Multicollinearity tests are performed in terms of the Variance Inflation Factor (VIF) and only models which do not present any factor with $VIF \geq 4$ are included among those to be selected (see Sec. SI 10A). The estimated coefficients reported in the main manuscript are those referring to the policy covariates and are estimated on the period starting from April 11th, 2020, and spanning until January 1st, 2021. Extensive robustness testing is performed to ensure the results' reliability. In Sec. SI 10B, we show parameter estimates for the different

policy covariates performing the regression i) over a different time window, and ii) excluding from the regression one country at a time (to ensure stability over country selection). We refer to Sec. SI 10 for more details on the model. It is important to stress that the adopted framework accounts for inter-country and inter-wealth-group differences using both standardized covariates and target variables for each country and wealth group.

While other modeling techniques –such as diff-in-diff and event studies– can provide stronger causality claims on the effect of policies on group behavior, the choice of modeling mobility behavior using a panel regression model is motivated by the fact that (i) selecting non-overlapping events and (ii) finding a reliable “untreated” reference population is not possible with policies being enacted/revoked in concomitant periods and with the continuously changing underlying epidemiological situation. Modeling group behavior in terms of a linear combination of epidemiological conditions and intensity of containment policies partially solves these issues allowing for an in-depth analysis of the association between different policy types and individual behavioral responses. Nevertheless, it is important to stress that the results obtained with this approach cannot be interpreted as causal relations between the outcome variable and its covariates.

Author contributions

L.L. and S.F. conceived the original idea and planned the experiments. A.C., A.M. provided geographical and demographic information. L.L., O.L.C., L.C., and L.M. processed the mobility data and carried out the experiments. L.L., O.L.C., B.L., N.L.G, and S.F. contributed to the interpretation of the results and wrote the manuscript.

Competing Interests

The authors declare no competing interests.

Acknowledgements

L.L. thanks G.K. for the insightful discussions and for his support during the entire project development. L.L. has been supported by the ERC project “IMMUNE” (Grant agreement ID: 101003183). The findings, interpretations, and conclusions expressed in this paper are entirely those of the authors. They do not necessarily represent the views of the International Bank for Reconstruction and Development/World Bank and its affiliated organizations, or those of the Executive Directors of the World Bank or the governments they represent.

References

- [1] Tian, H., Liu, Y., Li, Y., Wu, C.-H., Chen, B., Kraemer, M.U., Li, B., Cai, J., Xu, B., Yang, Q., *et al.*: An investigation of transmission control measures during the first 50 days of the covid-19 epidemic in china. *Science* **368**(6491), 638–642 (2020)
- [2] Gatto, M., Bertuzzo, E., Mari, L., Miccoli, S., Carraro, L., Casagrandi, R., Rinaldo, A.: Spread and dynamics of the covid-19 epidemic in italy: Effects of emergency

containment measures. *Proceedings of the National Academy of Sciences* **117**(19), 10484–10491 (2020)

- [3] Chinazzi, M., Davis, J.T., Ajelli, M., Gioannini, C., Litvinova, M., Merler, S., Piontti, A.P., Mu, K., Rossi, L., Sun, K., *et al.*: The effect of travel restrictions on the spread of the 2019 novel coronavirus (covid-19) outbreak. *Science* **368**(6489), 395–400 (2020)
- [4] Kraemer, M.U.G., Yang, C.-H., Gutierrez, B., Wu, C.-H., Klein, B., Pigott, D.M., Plessis, L., Faria, N.R., Li, R., Hanage, W.P., Brownstein, J.S., Layman, M., Vesprignani, A., Tian, H., Dye, C., Pybus, O.G., Scarpino, S.V.: The effect of human mobility and control measures on the covid-19 epidemic in china. *Science* **368**(6490), 493–497 (2020) <https://doi.org/10.1126/science.abb4218>
- [5] Perra, N.: Non-pharmaceutical interventions during the covid-19 pandemic: A review. *Physics Reports* **913**, 1–52 (2021)
- [6] Lucchini, L., Centellegher, S., Pappalardo, L., Gallotti, R., Privitera, F., Lepri, B., De Nadai, M.: Living in a pandemic: changes in mobility routines, social activity and adherence to covid-19 protective measures. *Scientific reports* **11**(1), 1–12 (2021)
- [7] Pullano, G., Valdano, E., Scarpa, N., Rubrichi, S., Colizza, V.: Evaluating the effect of demographic factors, socioeconomic factors, and risk aversion on mobility during the covid-19 epidemic in france under lockdown: a population-based study. *The Lancet Digital Health* **2**(12), 638–649 (2020) [https://doi.org/10.1016/S2589-7500\(20\)30243-0](https://doi.org/10.1016/S2589-7500(20)30243-0)
- [8] Woskie, L.R., Hennessy, J., Espinosa, V., Tsai, T.C., Vispute, S., Jacobson, B.H., Cattuto, C., Gauvin, L., Tizzoni, M., Fabrikant, A., Gadepalli, K., Boulanger, A., Pearce, A., Kamath, C., Schlosberg, A., Stanton, C., Bavadekar, S., Abueg, M., Hogue, M., Oplinger, A., Chou, K., Corrado, G., Shekel, T., Jha, A.K., Wellenius, G.A., Gabrilovic, E.: Early social distancing policies in europe, changes in mobility & covid-19 case trajectories: Insights from spring 2020. *PloS ONE* **16**(6), 0253071 (2021)
- [9] Lai, S., Ruktanonchai, N.W., Zhou, L., Prosper, O., Luo, W., Floyd, J.R., Wesolowski, A., Santillana, M., Zhang, C., Du, X., Yu, H., Tatem, A.J.: Effect of non-pharmaceutical interventions to contain COVID-19 in china. *Nature* **585**(7825), 410–413 (2020) <https://doi.org/10.1038/s41586-020-2293-x>
- [10] Nouvellet, P., Bhatia, S., Cori, A., Ainslie, K.E.C., Baguelin, M., Bhatt, S., Boonyasiri, A., Brazeau, N.F., Cattarino, L., Cooper, L.V., Coupland, H., Cucunuba, Z.M., Cuomo-Dannenburg, G., Dighe, A., Djaafara, B.A., Dorigatti, I., Eales, O.D., Elsland, S.L., Nascimento, F.F., FitzJohn, R.G., Gaythorpe, K.A.M., Geidelberg, L., Green, W.D., Hamlet, A., Hauck, K., Hinsley, W., Imai, N., Jeffrey, B., Knock, E., Laydon, D.J., Lees, J.A., Mangal, T., Mellan, T.A., Nedjati-Gilani, G., Parag, K.V., Pons-Salort, M., Ragonnet-Cronin, M., Riley, S., Unwin, H.J.T., Verity, R., Vollmer, M.A.C., Volz, E., Walker, P.G.T., Walters, C.E., Wang, H., Watson, O.J., Whittaker, C., Whittles, L.K., Xi, X., Ferguson, N.M., Donnelly, C.A.: Reduction in mobility and covid-19 transmission. *Nature Communications* **12**(1090) (2021)

- [11] Checo, A., Grigoli, F., Mota, J.M.: Assessing targeted containment policies to fight covid-19. *The BE Journal of Macroeconomics* **22**(1), 159–196 (2022)
- [12] Fudolig, M.I.D., Monsivais, D., Bhattacharya, K., Jo, H.-H., Kaski, K.: Internal migration and mobile communication patterns among pairs with strong ties. *EPJ Data Science* **10**(1), 16 (2021)
- [13] Alexander, L., Jiang, S., Murga, M., González, M.C.: Origin–destination trips by purpose and time of day inferred from mobile phone data. *Transportation research part c: emerging technologies* **58**, 240–250 (2015)
- [14] Jiang, S., Ferreira, J., Gonzalez, M.C.: Activity-based human mobility patterns inferred from mobile phone data: A case study of singapore. *IEEE Transactions on Big Data* **3**(2), 208–219 (2017)
- [15] Aleta, A., Martin-Corral, D., Piontti, A., Ajelli, M., Litvinova, M., Chinazzi, M., Dean, N.E., Halloran, M.E., Longini Jr, I.M., Merler, S., *et al.*: Modelling the impact of testing, contact tracing and household quarantine on second waves of covid-19. *Nature Human Behaviour* **4**(9), 964–971 (2020)
- [16] Yabe, T., Jones, N.K., Rao, P.S.C., Gonzalez, M.C., Ukkusuri, S.V.: Mobile phone location data for disasters: A review from natural hazards and epidemics. *Computers, Environment and Urban Systems* **94**, 101777 (2022)
- [17] Aleta, A., Martin-Corral, D., Bakker, M.A., Piontti, A., Ajelli, M., Litvinova, M., Chinazzi, M., Dean, N.E., Halloran, M.E., Longini Jr, I.M., et al.: Quantifying the importance and location of sars-cov-2 transmission events in large metropolitan areas. *Proceedings of the National Academy of Sciences* **119**(26) (2022)
- [18] Pangallo, M., Aleta, A., Chanona, R., Pichler, A., Martin-Corral, D., Chinazzi, M., Lafond, F., Ajelli, M., Moro, E., Moreno, Y., et al.: The unequal effects of the health-economy tradeoff during the covid-19 pandemic. *arXiv preprint arXiv:2212.03567* -(- (2022)
- [19] Jia, J.S., Lu, X., Yuan, Y., Xu, G., Jia, J., Christakis, N.A.: Population flow drives spatio-temporal distribution of covid-19 in china. *Nature* **582**(7812), 389–394 (2020) <https://doi.org/10.1038/s41586-020-2284-y>
- [20] Grantz, K.H., Meredith, H.R., Cummings, D.A., Metcalf, C.J.E., Grenfell, B.T., Giles, J.R., Mehta, S., Solomon, S., Labrique, A., Kishore, N., *et al.*: The use of mobile phone data to inform analysis of covid-19 pandemic epidemiology. *Nature communications* **11**(1), 1–8 (2020)
- [21] Bonaccorsi, G., Pierri, F., Cinelli, M., Flori, A., Galeazzi, A., Porcelli, F., Schmidt, A.L., Valensise, C.M., Scala, A., Quattrociocchi, W., Pammolli, F.: Economic and social consequences of human mobility restrictions under covid-19. *Proceedings of the National Academy of Sciences* **117**(27), 15530–15535 (2020)

[22] Serajuddin, U., Hamadeh, N.: New World Bank country classifications by income level: 2020-2021. Accessed on 2021-08-28 (2020). <https://blogs.worldbank.org/opendata/new-world-bank-country-classifications-income-level-2020-2021> Accessed 2021-08-28

[23] Paul, A., Englert, P., Varga, M.: Socio-economic disparities and covid-19 in the usa. *Journal of Physics: Complexity* **1**(1), 00 (2021)

[24] Jay, J., Bor, J., Nsoesie, E.O., Lipson, S.K., Jones, D.K., Galea, S., Raifman, J.: Neighbourhood income and physical distancing during the covid-19 pandemic in the united states. *Nature human behaviour* **4**(12), 1294–1302 (2020)

[25] Gauvin, L., Bajardi, P., Pepe, E., Lake, B., Privitera, F., Tizzoni, M.: Socio-economic determinants of mobility responses during the first wave of covid-19 in italy: from provinces to neighbourhoods. *Journal of the Royal Society Interface* **18**(181) (2021)

[26] Blundell, R., Costa Dias, M., Joyce, R., Xu, X.: Covid-19 and inequalities. *Fiscal studies* **41**(2), 291–319 (2020)

[27] Bambra, C., Riordan, R., Ford, J., Matthews, F.: The covid-19 pandemic and health inequalities. *J Epidemiol Community Health* **74**(11), 964–968 (2020)

[28] Dorn, A.v., Cooney, R.E., Sabin, M.L.: Covid-19 exacerbating inequalities in the us. *Lancet* **395**(10232), 1243–1244 (2020)

[29] Abedi, V., Olulana, O., Avula, V., Chaudhary, D., Khan, A., Shahjouei, S., Li, J., Zand, R.: Racial, economic, and health inequality and covid-19 infection in the united states. *J. Racial and Ethnic Health Disparities* **8**, 732–742 (2021)

[30] Maloney, W.F., Taskin, T.: Determinants of social distancing and economic activity during covid-19: A global view. *World Bank Policy Research Working Paper* **1**(9242), 00 (2020)

[31] Kephart, J.L., Delclòs-Alió, X., Rodríguez, D.A., Sarmiento, O.L., Barrientos-Gutiérrez, T., Ramirez-Zea, M., Quistberg, D.A., Bilal, U., Roux, A.V.D.: The effect of population mobility on covid-19 incidence in 314 latin american cities: a longitudinal ecological study with mobile phone location data. *The Lancet Digital Health* **1**(1), 00 (2021)

[32] Gozzi, N., Tizzoni, M., Chinazzi, M., Ferres, L., Vespignani, A., Perra, N.: Estimating the effect of social inequalities on the mitigation of covid-19 across communities in santiago de chile. *Nature Communications* **12**(1), 1–9 (2021)

[33] Heroy, S., Loaiza, I., Pentland, A., O’Clery, N.: Covid-19 policy analysis: labour structure dictates lockdown mobility behaviour. *Journal of the Royal Society Interface* **18**(176), 20201035 (2021)

[34] Mena, G.E., Martinez, P.P., Mahmud, A.S., Marquet, P.A., Buckee, C.O., Santillana, M.: Socioeconomic status determines covid-19 incidence and related mortality in santiago, chile. *Science* **372**(6545) (2021)

[35] Garrote Sanchez, D., Gomez Parra, N., Ozden, C., Rijkers, B., Viollaz, M., Winkler, H.: Who on earth can work from home? *The World Bank Research Observer* **36**(1), 67–100 (2021)

[36] Dingel, J.I., Neiman, B.: How many jobs can be done at home? *Journal of Public Economics* **189**, 104235 (2020)

[37] Veraset: Veraset Movement Data – Veraset. Accessed on 2021-02-17. <https://www.veraset.com/products/movement/> Accessed 2021-02-17

[38] McKenzie, D.J.: Measuring inequality with asset indicators. *Journal of population economics* **18**(2), 229–260 (2005)

[39] Coven, J., Gupta, A., Yao, I.: Jue insight: Urban flight seeded the covid-19 pandemic across the united states. *Journal of urban economics* -, 103489 (2022) <https://doi.org/10.1016/j.jue.2022.103489>

[40] Chetty, R., Friedman, J.N., Hendren, N., Stepner, M., et al.: The economic impacts of covid-19: Evidence from a new public database built using private sector data. Technical report, national Bureau of economic research (2020)

[41] Mongey, S., Pilossoph, L., Weinberg, A.: Which workers bear the burden of social distancing? *The Journal of Economic Inequality* **19**, 509–526 (2021)

[42] Data, O.W.I.: Our World in Data - COVID-19 Public Data. github. Accessed on 2023-02-01. <https://github.com/owid/covid-19-data/tree/master/public/data> Accessed 2023-02-01

[43] Hale, T., Webster, S., Anna, P., Toby, P., Beatriz, K.: Oxford covid-19 government response tracker. Blavatnik school of government working paper **31**, 2020–11 (2020)

[44] Bank, T.W.: World Development Report 2021: Data for Better Lives. The World Bank, 1818 H Street, N.W. Washington, DC 20433 USA (2021)

[45] Fraiberger, S.P., Astudillo, P., Candeago, L., Chunet, A., Jones, N.K.W., Khan, M.F., Lepri, B., Gracia, N.L., Lucchini, L., Massaro, E., Montfort, A.: Uncovering socioeconomic gaps in mobility reduction during the COVID-19 pandemic using location data (2020)

[46] Vyass, S., Kumaranayake, L.: Constructing socioeconomic status indexes: how to use principal component analysis. *Health Policy Plan* **21**(6), 459–68 (2006)

[47] Csáji, B.C., Browet, A., Traag, V.A., Delvenne, J.-C., Huens, E., Van Dooren, P., Smoreda, Z., Blondel, V.D.: Exploring the mobility of mobile phone users. *Physica A: Statistical Mechanics and its Applications* **533**, 122182 (2019)

statistical mechanics and its applications **392**(6), 1459–1473 (2013)

- [48] Çolak, S., Alexander, L.P., Alvim, B.G., Mehndiratta, S.R., González, M.C.: Analyzing cell phone location data for urban travel: current methods, limitations, and opportunities. *Transportation Research Record* **2526**(1), 126–135 (2015)
- [49] Pappalardo, L., Ferres, L., Sacasa, M., Cattuto, C., Bravo, L.: An individual-level ground truth dataset for home location detection. *arXiv preprint arXiv:2010.08814* **2010**(08814), 1–20 (2020)
- [50] Song, C., Koren, T., Wang, P., Barabási, A.-L.: Modelling the scaling properties of human mobility. *Nature physics* **6**(10), 818–823 (2010)
- [51] Barbosa, H., Lima-Neto, F.B., Evsukoff, A., Menezes, R.: The effect of recency to human mobility. *EPJ Data Science* **4**(1), 1–14 (2015)
- [52] Oliver, N., Lepri, B., Sterly, H., Lambiotte, R., Delestatte, S., De Nadai, M., Letouzé, E., Salah, A.A., Benjamins, R., Cattuto, C., *et al.*: Mobile phone data for informing public health actions across the covid-19 pandemic life cycle. *Science Advances* **6**(23), 0764 (2020)
- [53] Wesolowski, A., Buckee, C.O., Engø-Monsen, K., Metcalf, C.J.E.: Connecting mobility to infectious diseases: the promise and limits of mobile phone data. *The Journal of infectious diseases* **214**(suppl_4), 414–420 (2016)

1 **Socioeconomic disparities in mobility behavior during the COVID-19 pandemic in**
2 **developing countries**

3 Lorenzo Lucchini,^{1,2,3,4} Ollin D. Langle-Chimal,^{3,5} Lorenzo Candeago,³ Lucio Melito,³ Alex
4 Chunet,³ Aleister Montfort,³ Bruno Lepri,⁴ Nancy Lozano Gracia,³ and Samuel Fraiberger³

5 ¹*Centre for Social Dynamics and Public Policy, Bocconi University, Milan 20100, Italy*

6 ²*Institute for Data Science and Analytics, Bocconi University, Milan 20100, Italy*

7 ³*World Bank, Washington - DC*

8 ⁴*Fondazione Bruno Kessler, Trento - Italy*

9 ⁵*University of Vermont, Burlington - VT*

10

SUPPLEMENTARY INFORMATION

11

SI 1. FROM GPS DATA AND TO MOBILITY PATTERNS

12 This section provides supplementary information about the data used in our analyses. The data provider,
 13 Veraset, is an SDK aggregator working all around the globe, collecting GPS mobility traces from personal
 14 devices of individuals' who opted-in to their services. In our analyses we focus on middle-income countries
 15 from different geographical areas.

16

SI 2. USER DISTRIBUTION

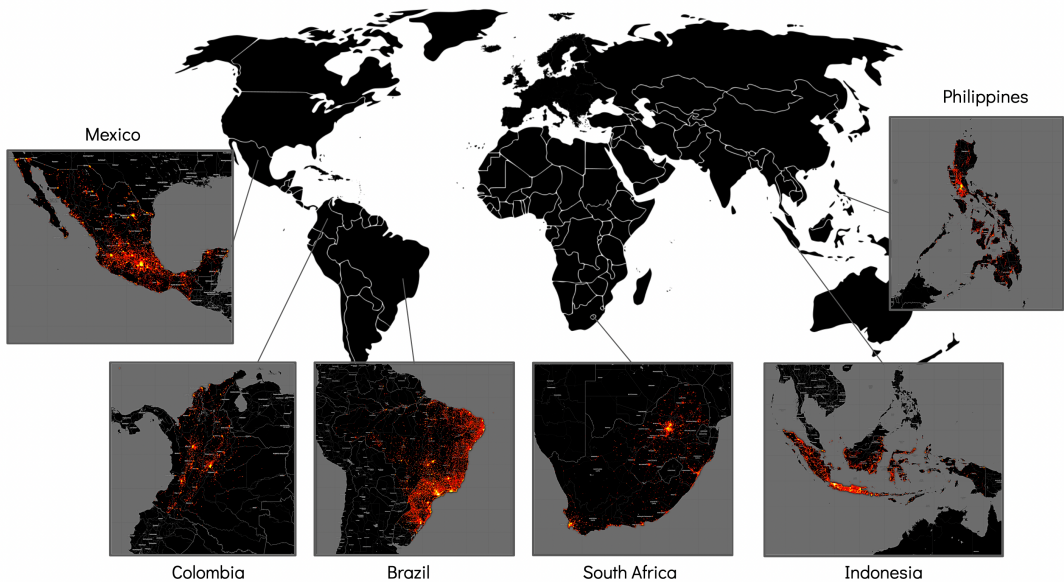


Figure SI 1. User distribution across the 6 countries.

17 We select 6 middle-income countries and follow individuals' trajectories over a time span of almost
 18 one year (2020). The selected countries are: Brazil, Colombia, Indonesia, Mexico, Philippines and South
 19 Africa. The largest bulk of these users lays on the urban/metropolitan areas of the main cities of each
 20 country. Figure SI 1 shows the geographical distribution of the GPS points registered from the users'
 21 personal devices.

22

SI 3. MOBILITY DATA PROCESSING DETAILS

23

A. From pings to stop events

24 The first step aims at aggregating pings into consecutive group of pings called “stop events”. To this
 25 end, previous work [2, 9] has shown how, starting from GPS trajectories, it is possible to aggregate the
 26 information in terms of a series of stops an individual performed. In this perspective, stop events filter
 27 inaccurate GPS points and discard non-stationary events from the series [1, 9].

28 Schematically, in this first step the following actions are performed:

29 1. A rough filter on accuracy is performed to exclude pings with inconsistent or too large accuracy
 30 values, i.e. $accuracy \geq 0m$ and $accuracy \leq 200m$.

31 2. A second filter is performed by checking coordinates values and constraining them to the latitude
 32 and longitude domain, i.e. $-90 \leq lat \leq 90$ and $-180 \leq lon \leq 180$.

33 3. Third, we only kept pings that were timestamped within the temporal period of days Veraset provided.
 34 Pings with timestamp outside the temporal window are potentially introduced by delays in the upload
 35 process.

36 4. We then discarded all users which were not significantly active during the validation period.

37 We then define a “stop event” as a consecutive sequence of pings for which the distance between each
 38 pair of pings is smaller than $r = 25m$. We additionally require that the maximum time between two
 39 consecutive pings of the sequence should be less than 1 hour for the sequence to be considered part of the
 40 same stop event. Similarly, we fix the minimum distance between the earliest time of a candidate stop event
 41 and the latest to be at least 5 minutes. To each stop event we associate a *lat-lon* tuple based on the medoid
 42 of the latitude and longitude of the pings forming the stop event. After this processing, stop events with an
 43 average pings’ accuracy greater than $100m$ are discarded as an additional quality requirement.

44 To each stop event is then associated a unique “GEOMID”, representing a unique administrative unit in
 45 the *administrative boundaries dataset* by means of the *H3 library* [13] and *Apache Sedona* [14].

46

B. From stop events to stop locations

47 This second step applies a clustering algorithm (we adopted the DBSCAN [7] algorithm) to all the stop
 48 events of a single individual. This results in an assignment to each stop event of a label identifying all other
 49 stop events clustered together by the algorithm. We call the label of each stop event “stop location”.

50

C. Home and work locations

51 Reliable home and work identification algorithms are essential to map an individual’s mobile phone data
 52 trace to their socioeconomic background. During the past decades several efforts had been made in order to
 53 correctly assign such labels to a coordinate pair for a single user [1, 5, 6, 10]. In this work, we build upon
 54 the preferential return mechanism based on the exploration/exploitation dichotomy [3, 11] segmenting by
 55 important heuristics such as the day of the week and visiting hours.

56 Given that we are interested in changes in the users’ primary homes, we propose a pipeline to define and
 57 optimize the labeling of a given cluster or stop location as a possible home or work defined dynamically.
 58 In order to do this, we define thresholds with the minimum amount of days when the cluster is visited
 59 (*min_periods_over_window*) over a rolling window of days (*period_window*). We use two different sets of
 60 these parameters to define both home and work. The difference between the labels is given by the heuristics
 61 of plausible times when a user might be present at that given location.

62 With this in mind, we firstly define nighttime as the period of hours comprised by the time between
 63 11pm and 5am of the following day. The rest of the day will be marked as daytime. We also consider a
 64 working day to be Monday to Friday while leaving Saturday and Sunday as weekends. Then, we define
 65 as home candidates those stop clusters that are visited on weekends or during “nighttime” and as work
 66 candidates those visited during the complementary hours of the week. We add an extra restriction to work
 67 by setting a minimum amount of average time per day spent there. When the candidates are computed all
 68 the “work” labels are kept while only the most frequently visited “home” within the window is considered
 69 as such. The remaining clusters are then labeled as “other”. Labels are assigned dynamically, meaning that,
 70 in each time-window, we look to a user’s home location and work locations independently. However, if a
 71 stop location is labelled as either home or work location at least once, i.e. in at least one time-window, we
 72 expand the labelling to all visit ever performed by the user to that location, since it is likely to be always
 73 related to residence or work activity conducted before or after it’s classification.

74

D. Activity filter

75 Following the same perspective, aiming at providing a reliable and long term dataset of individuals to
 76 which a socioeconomic status can be assigned, additional filters on the minimum level of activity for each
 77 individual are applied. The idea is to perform the analysis on a set of individuals which remain active up to a
 78 minimum level, to ensure a minimum longitudinal coverage and thus ensure a sufficient level of significance
 79 for the computed metrics. More specifically, these filters require i) a minimum number of days of activity

80 before the beginning of March 2020, and ii) a minimum level of activity after the beginning of March 2020
81 and before the end of the user records. Here an individual is defined to be active on a day if she/he has at
82 least one stop event recorded on that day. The “minimum level” of activity is defined as a 20% day threshold
83 over each of the two periods separately.

84 For the specific case of the Republic of Indonesia, the period before the pandemic starts at the beginning
85 of February 2020 to avoid the inclusions of individuals which were later pulled out due to a major customer
86 dropout. The “during pandemic” period remains unchanged.

87 **SI 4. EXPANDING POLYGONS AND FILLING GAPS BETWEEN SMALLER ADMINISTRATIVE
88 UNITS**

89 High precision measurement of mobility patterns are difficult to connect to equally precise and fine-
90 grained demographic data. Our approach, as described in Material and Methods (section “Administrative
91 boundaries data”), leverages over local administrative data at the smaller administrative units for each coun-
92 try. Often, these data consists of polygons and summary demographics for the area contained within each
93 polygon. At the most finer level these polygons, i.e. administrative units’ boundaries, consists of blocks
94 and/or neighborhoods within cities. We take advantage of the geospatial data distributed by the statistical
95 agencies of each country, which makes it difficult to homologate the polygons at the sub-national level.
96 The highly precise registration of administrative polygons often neglects to include local streets and other
97 neighbouring elements of the city in favor of a more accurate representation of blocks and places of inter-
98 ests such as parks. Albeit being these polygons precise from an administrative perspective, they result in
99 an incomplete coverage of the city area. In the interest of connecting stop locations and demographic data,
100 the gaps between them are responsible for a partial spillover of the mobility data at our disposal. Being a
101 cluster location an object consisting of several stops happening at different times but in a restricted radius
102 area, they are sensitive to boundary effects ultimately induced by both the limited accuracy of GPS locations
103 and the stop and clustering processing. To reduce this loss of data, i.e. to assign an administrative unit also
104 to cluster locations which fall outside high-precision administrative borders, we expand these borders filling
105 the gap areas with the following approach. For each country, we first identify all the polygons surrounded to
106 empty space (i.e., those are the only ones to be expanded), and those which not. We merge all the polygons
107 without any gaps between them to create a country mask. Then, we repopulate the polygons to expand by
108 interpolating new spatial points every 2 meters; this step yield the same polygons but with denser borders
109 defining them. We use this each of these spatial points as centroids to generate a Voronoi tessellation using
110 the mask from the first step [4]. Finally we find all the Voronoi polygons that touch an original one and

¹¹¹ redefine the extent of the latter by the union of the former ones.

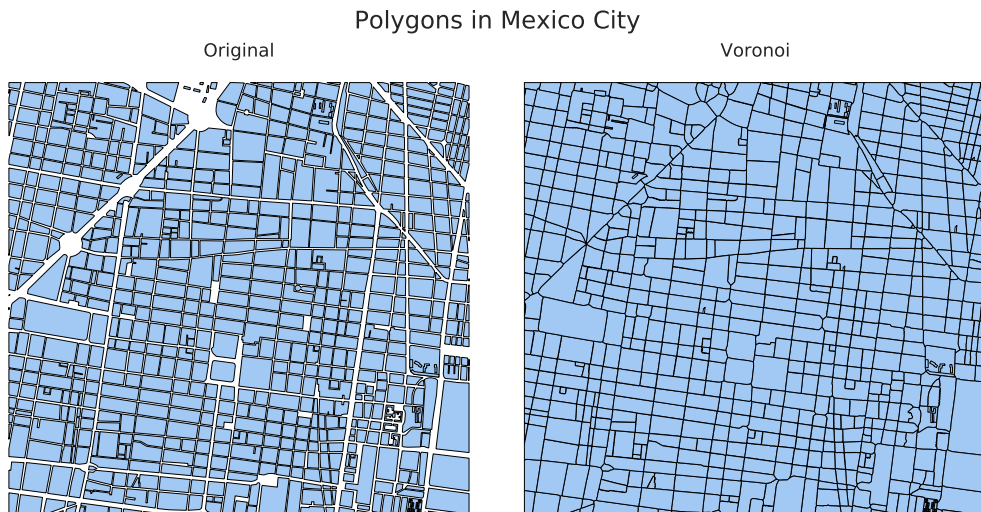


Figure SI 2. Polygon expansion of administrative units in urban areas.

¹¹²

SI 5. VALIDATION OF HOME/WORK STOP LOCATIONS PATTERNS

¹¹³ Particular care was devoted in this work to the classification of stop locations into “home” and “work”
¹¹⁴ locations. To produce reliable labels, a subset of devices’ trajectories was independently manually anno-
¹¹⁵ tated. Two independent annotators were asked to look at all the stop locations of 500 different users across
¹¹⁶ five different countries and label them as either “home”, or “work” or “other” locations. Annotators were
¹¹⁷ provided with information about nearby point of interests, satellite imagery and summary statistics about
¹¹⁸ each stop location. Point Of Interest (from both OpenStreetMap and Google Maps) and satellite imagery
¹¹⁹ (from Google Maps) were provided in the form of an explorable map. Summary statistics informed annota-
¹²⁰ tors about the fraction of time spent in a location daily spanning over the entire study period, the fraction of
¹²¹ time spent in different weekdays over the average week (this helped spotting weekday-weekend patterns),
¹²² and the fraction of time spent over different hours of a day for an average day of the year.

¹²³ The resulting labels of the two annotators were then compared and, when different opinions were ex-
¹²⁴ pressed, a third independent annotator was asked to tie-break selecting the best label.

¹²⁵ Performances were testes against the annotated labels to see how good the labelling algorithms is per-
¹²⁶ forming. Grid search exploration was used to check for different algorithm configurations, tuning five
¹²⁷ different parameters: time-window size for home location detection, time-window size for work location
¹²⁸ detection (*period_window*), the minimum number of day an individual visited a stop location within the

129 period window for both home and work location separately (*min periods over window*), and the minimum
 130 frequency of time an individual should spend at their workplaces to label those locations as work locations.
 131 Performances were tested by means of Cohen's Kappa test, reaching statistically comparable results, with
 132 up to 80% of agreement between algorithm and annotators for the best parameter configuration.

133

SI 6. DISTRIBUTION OF TIME SPENT

134 We find that for all of the studied countries the time spent at home locations was increased relative to a
 135 pre-pandemic baseline. This increment spans across different wealth groups. The location with the largest
 136 time spent reduction was the individual's work place. Interestingly, the high wealth users increased their
 137 time spent at home more than their low-wealth counterparts while they also reduced their time spent at
 138 work. In general the share of time spent at third locations was also reduced.

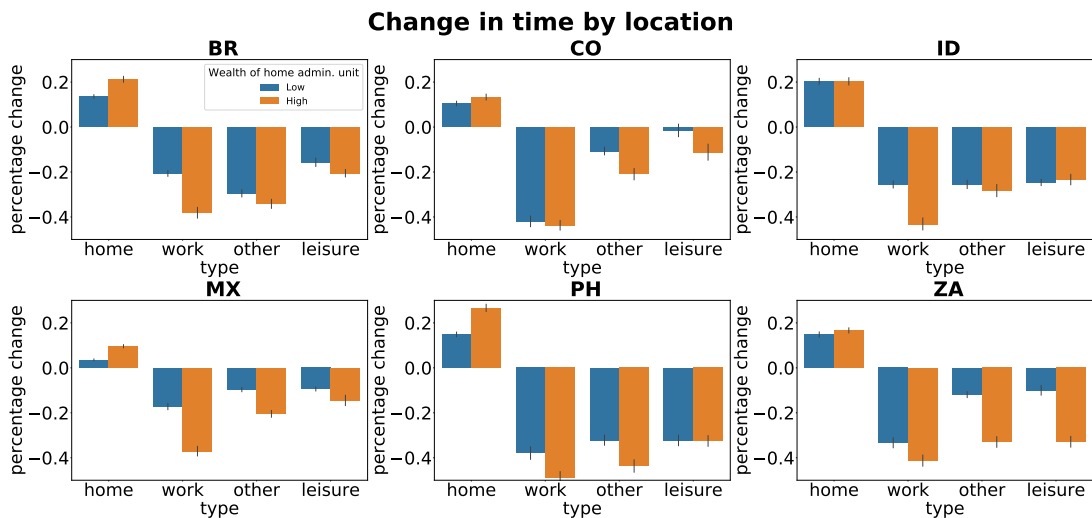


Figure SI 3. Percentage change of time spent by location.

139

SI 7. RESULTS BY CITY

140 In the main paper we show the aggregated results of users with the primary home location assigned to
 141 any of the 5 largest cities of each country. Figures [SI 4](#) and [SI 5](#) show the share of users not leaving their
 142 home and the share of users commuting to work only on the largest city of each country.

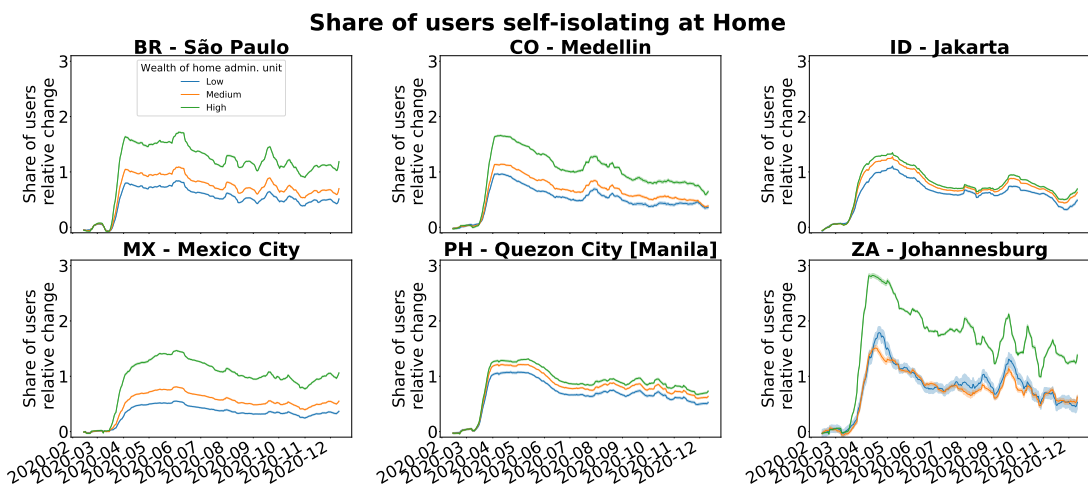


Figure SI 4. Percentage change of share of users isolating at home by wealth of administrative home unit in the largest city (by coverage).

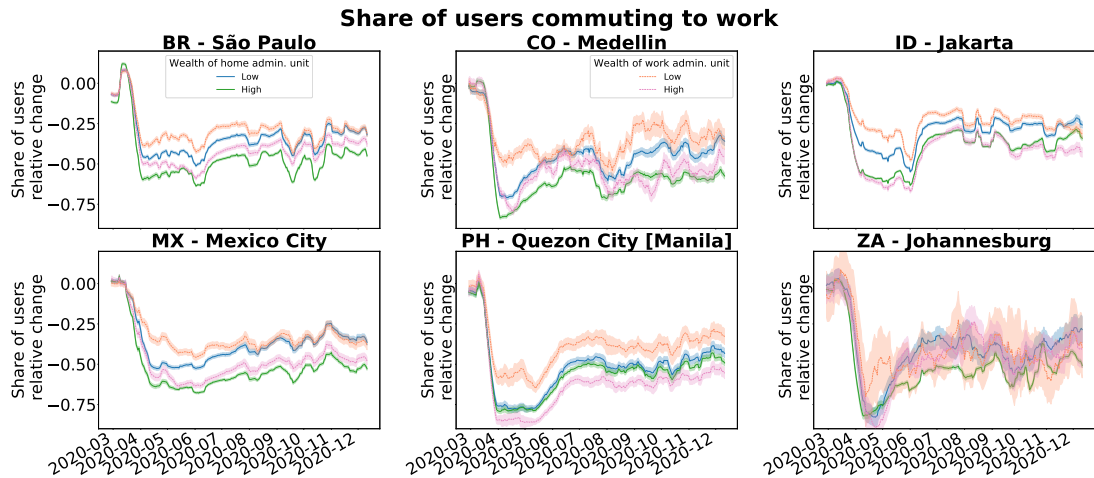


Figure SI 5. Percentage change of share of commuters by wealth of administrative home unit and low wealth commuters by wealth of administrative work unit in the largest city (by coverage).

143

SI 8. GAPS BETWEEN HIGH AND LOW INCOME GROUPS

144

This section illustrates directly the gaps between income groups over the entire time span of our analysis.

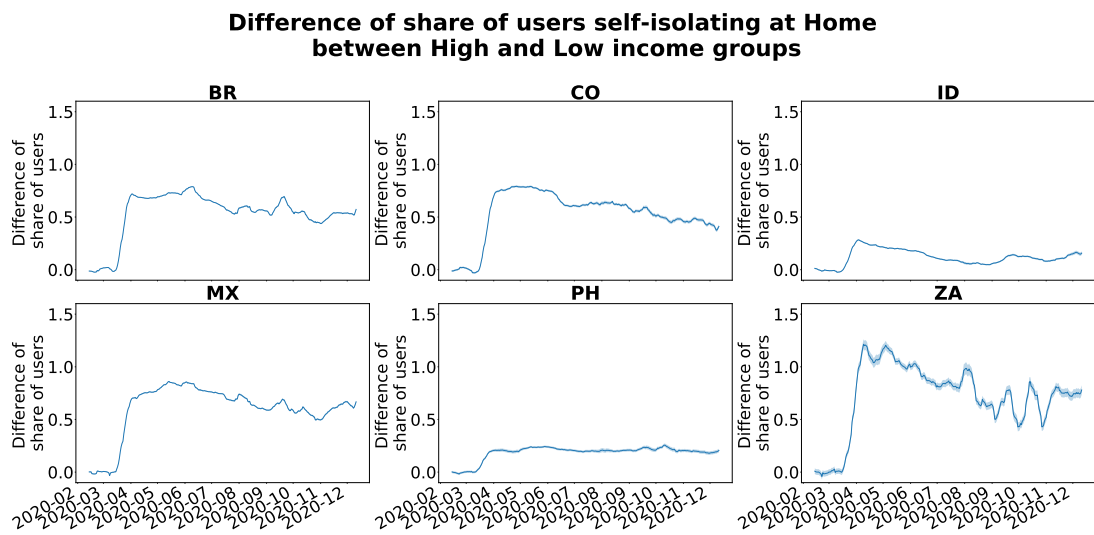


Figure SI 6. Difference of the percentage change of share of users self-isolating at home by wealth of administrative home unit in the whole country.

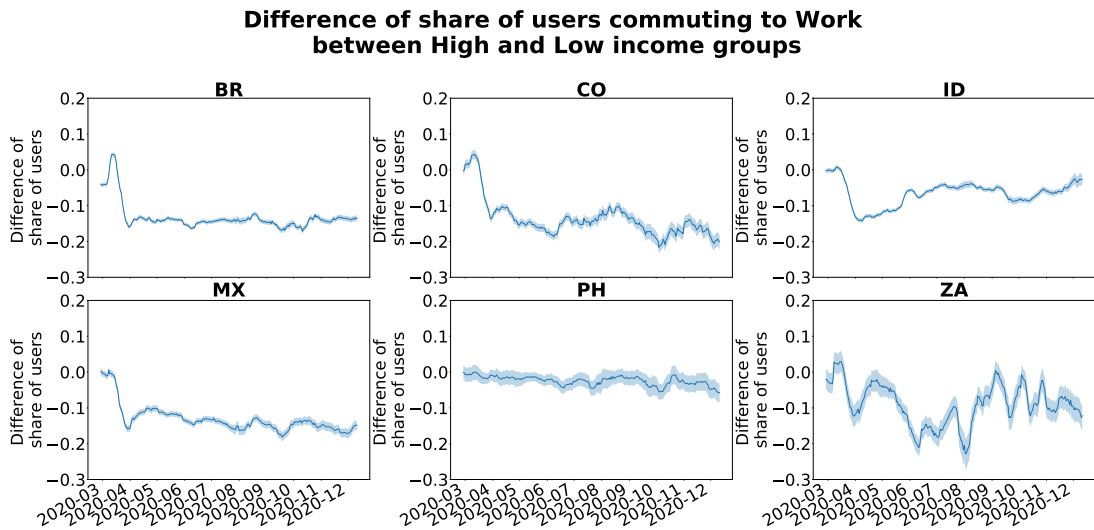


Figure SI 7. Difference of the percentage change of share of commuters by wealth of administrative home unit in the whole country.

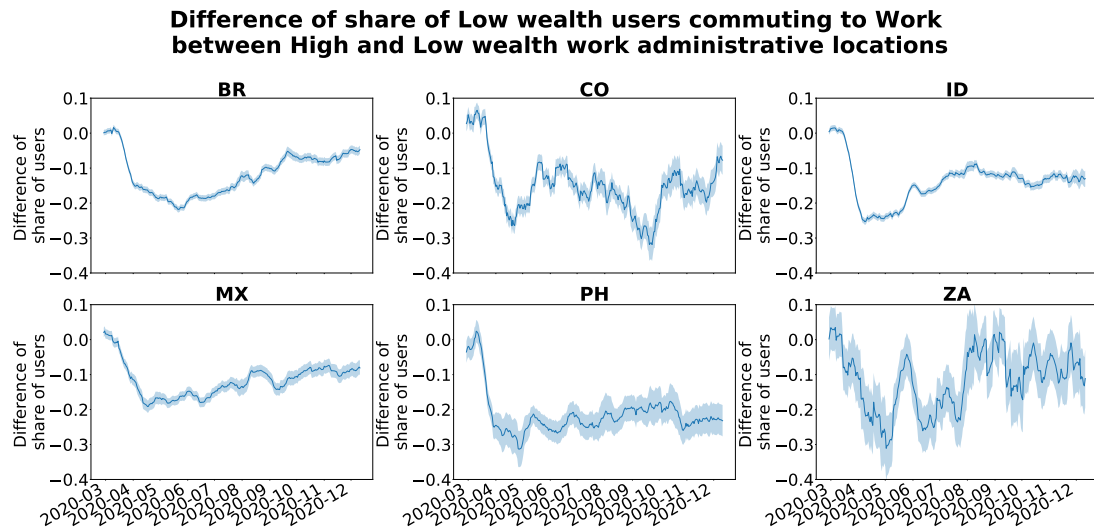


Figure SI 8. Difference of the percentage change of share of low wealth commuters by wealth of administrative work unit in the whole country.

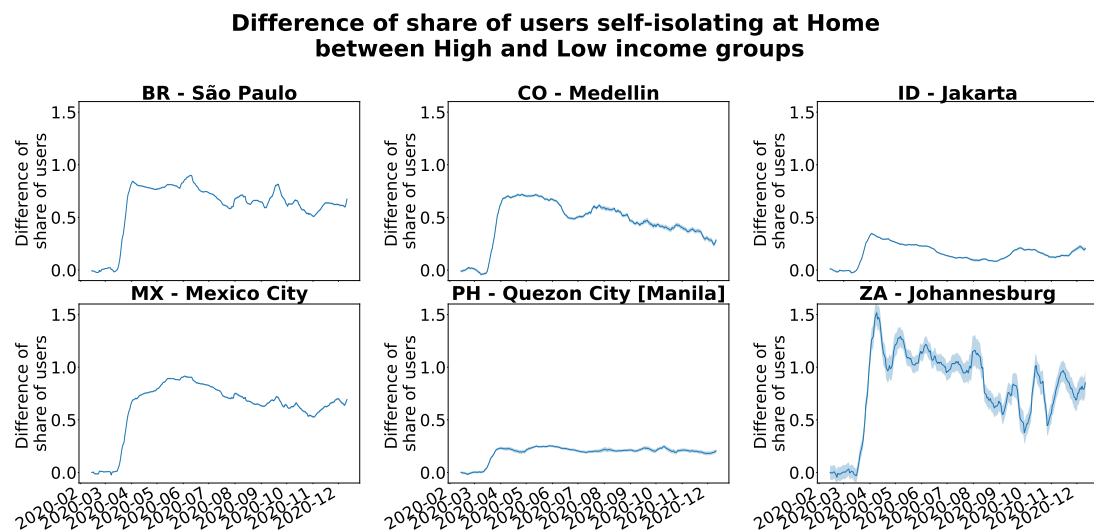


Figure SI 9. Difference of the percentage change of share of users self-isolating at home by wealth of administrative home unit in the largest city (by coverage).

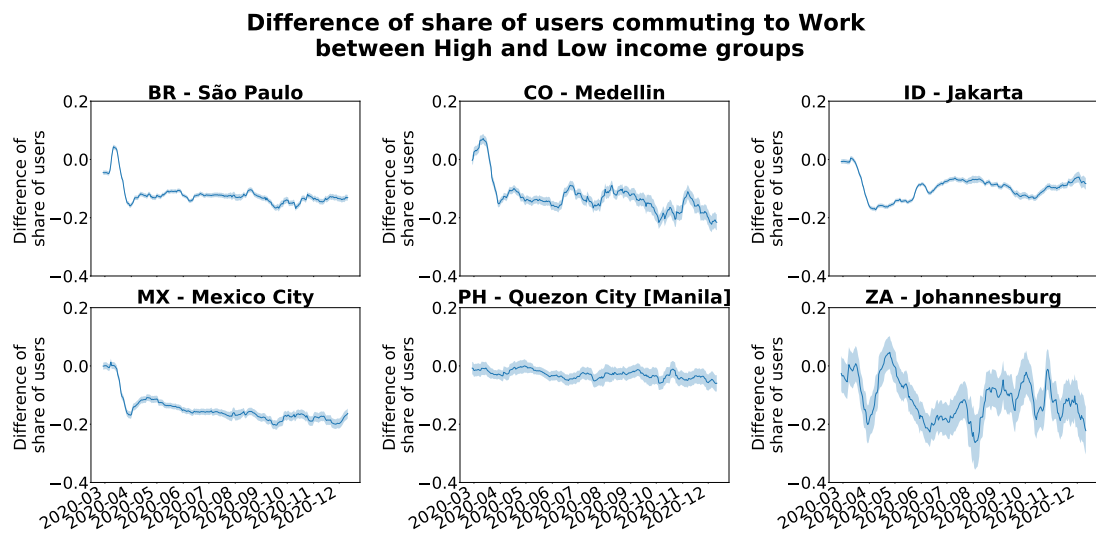


Figure SI 10. Difference of the percentage change of share of commuters by wealth of administrative home unit in the largest city (by coverage).

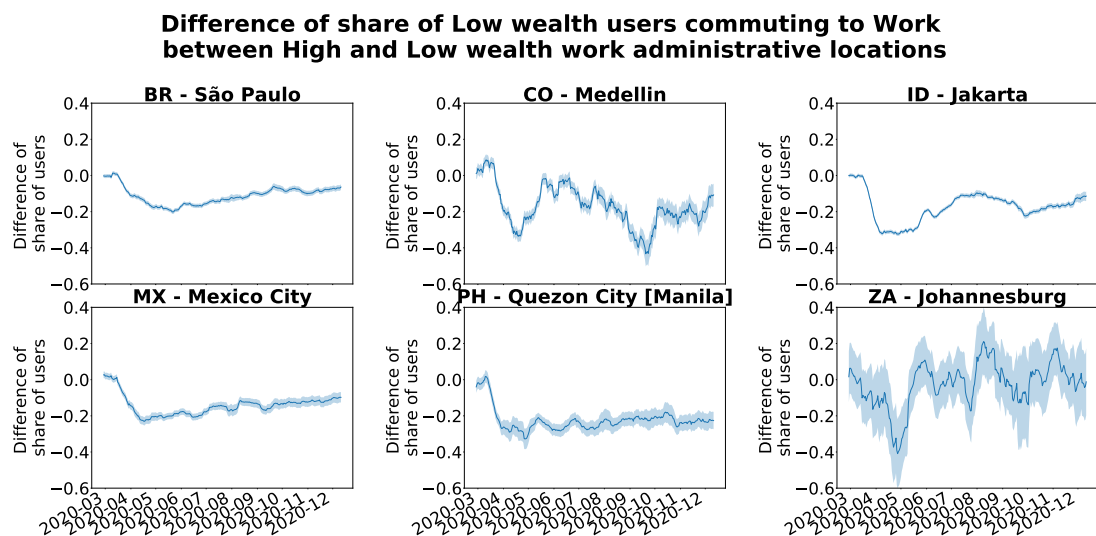


Figure SI 11. Difference of the percentage change of share of low wealth commuters by wealth of administrative work unit in the largest city (by coverage).

145

SI 9. MIGRATION PATTERNS

146 In the main text we discuss and present migration pattern from urban to rural areas. Here we show
 147 complementary migration patterns: cumulative migration curves from urban to rural (see Fig. SI 12), from
 148 rural to urban (see Fig. SI 13), and the net daily share of users migrating from urban to rural areas (see
 149 Fig. SI 14).

Cumulative share of users migrating to rural

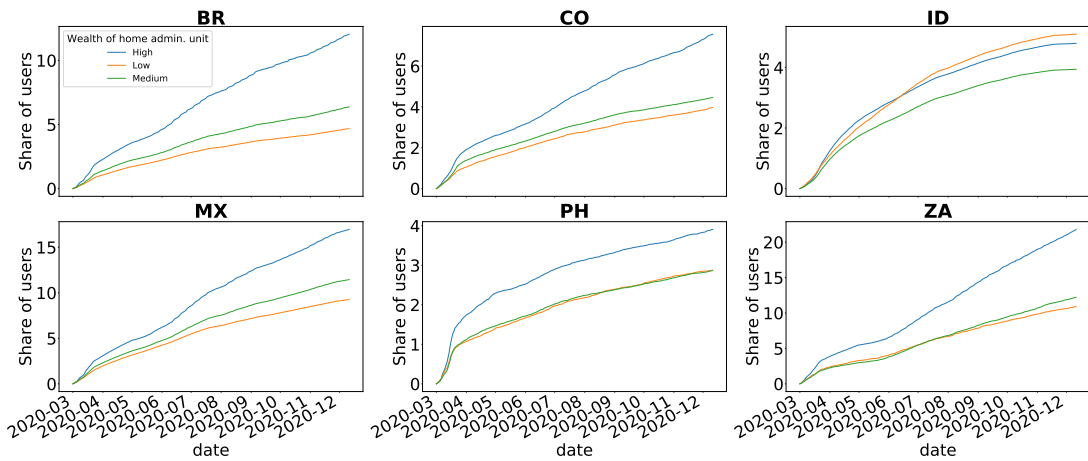


Figure SI 12. Cumulative share of users migrating from urban to rural areas.

Cumulative share of users migrating to urban

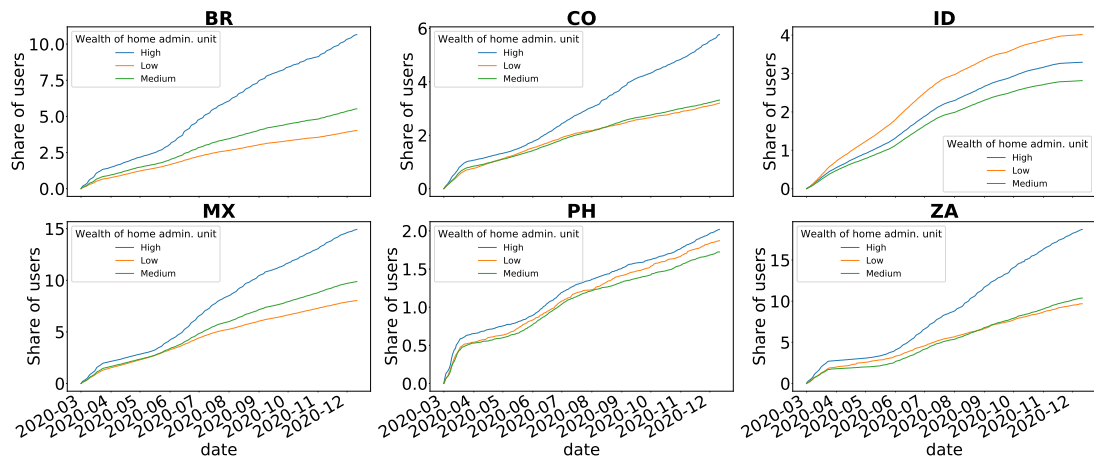


Figure SI 13. Cumulative share of users migrating from rural to urban areas.

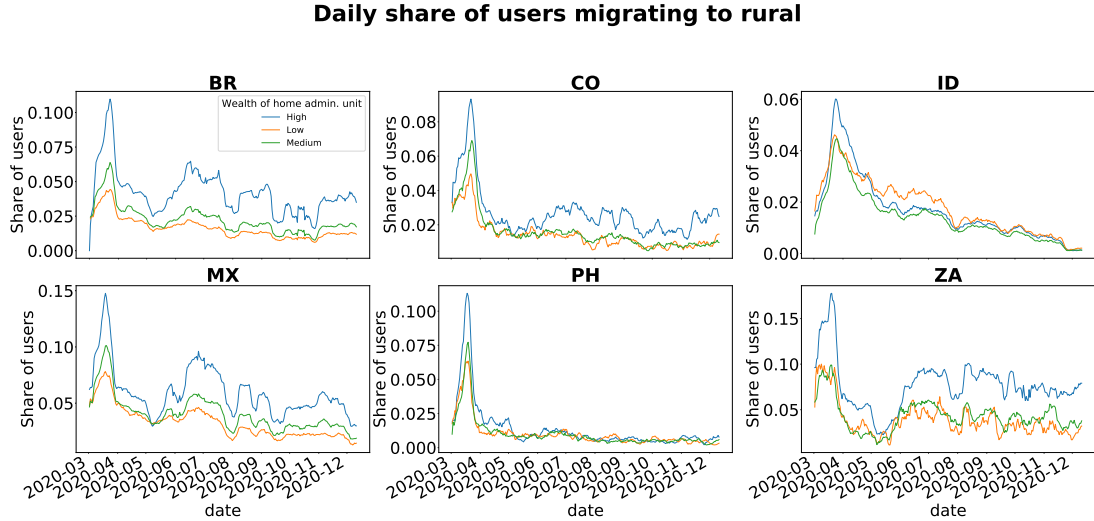


Figure SI 14. Daily share of users migrating from urban to rural areas.

150

SI 10. MOBILITY BEHAVIOUR AND POLICY INTERVENTIONS

151

A. Hierarchical model components selection

To provide policy-specific associations we first divide policies in three different categories as labelled by Hale et al. [8]: containment, economic, and health-related policies. Containment policies are those focused on reducing physical contacts among citizens: school, workplace, public transport closures, stay-at-home orders, and internal movements restrictions. Economic policies are those providing economic support to citizens either via debt-relief or income support. Health-related measures are those aimed at informing about safe behaviour (information campaigns), tracing and testing, and for other preventive behaviour, such as facial covering and protection of elderly people. Epidemiological quantities such as local cases incidence and local death incidence are included as covariates. The model configures as a panel regression model, where group-and-country specific mobility indicators are associated with local incidence and policy-categories indices. Following the same notation as in the main manuscript:

$$mb_{ic} = a_i * incidence_g \quad (1)$$

$$+ b_i * incidence_c \quad (2)$$

$$+ c_{i,contain} * C_{c,contain} \quad (3)$$

$$+ c_{i,economic} * C_{c,economic} \quad (4)$$

$$+ c_{i,health} * C_{c,health}; \quad (5)$$

152 We run a generalised-least-square regression to estimate model parameters and we compute the BIC as
 153 a metric for model performance comparison. We compare this model with simpler models, involving fewer
 154 covariates to only keep significant ones. In particular, we compare all possible combinations of the five
 155 covariates presented in Eq.1-4.

156 Figure SI 15 reports BIC values for all model combinations. All models that are included do not show
 157 significant multicollinearity. Multicollinearity is tested by means of the Variance Inflation Factor (VIF) and
 158 is required to be below 4 for each component in the model.

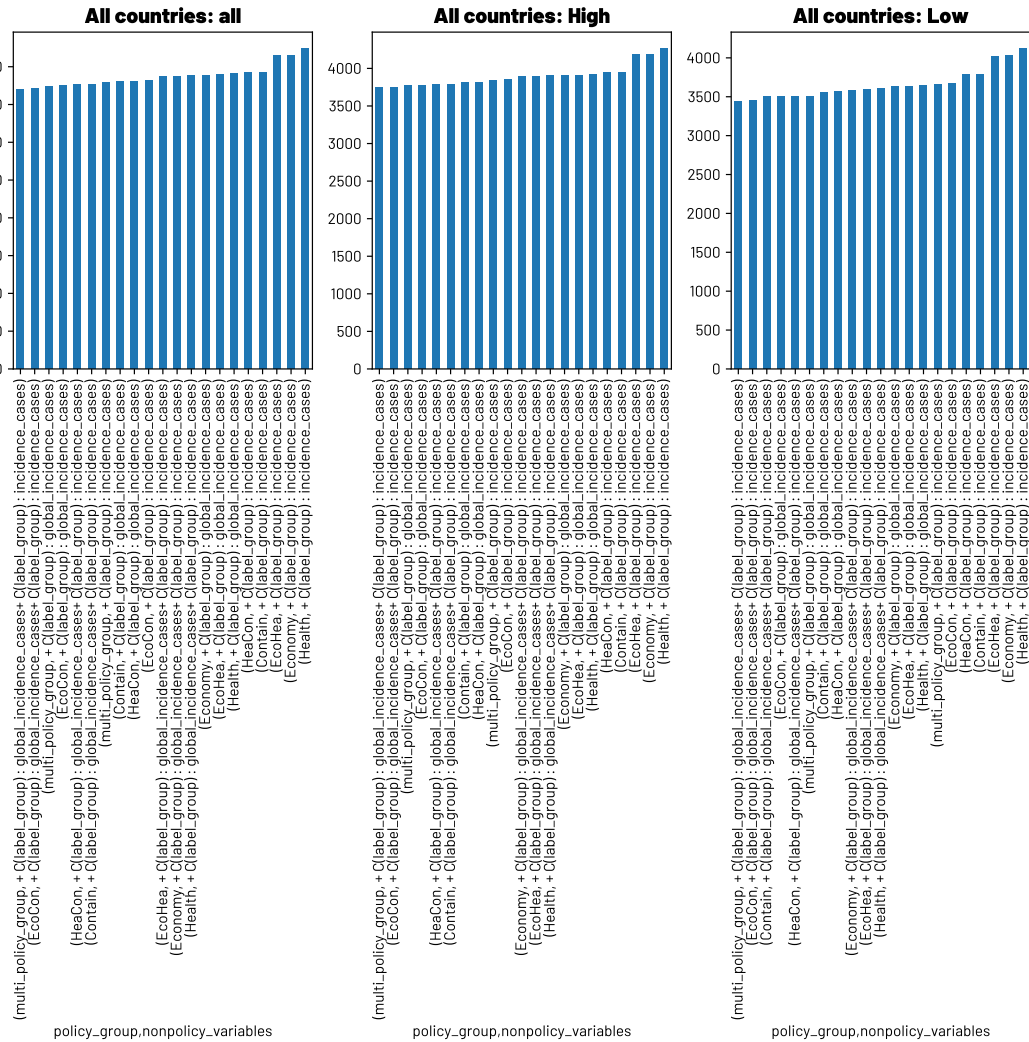


Figure SI 15. *BIC values for all model combinations that do not show any significant multicollinearity.* Each panel reports BIC values when modeling behaviour of “all” wealth groups (left), “high-wealth” group only (center), and “low-wealth” group only (right).

159 Further robustness testing is performed by regressing the models on single country data (see Fig. SI 16-
 160 SI 21). Consistent results are found, showing that both global incidence of cases, local incidence of cases,

¹⁶¹ and Containment policies plays a crucial role in modeling mobility behaviour.

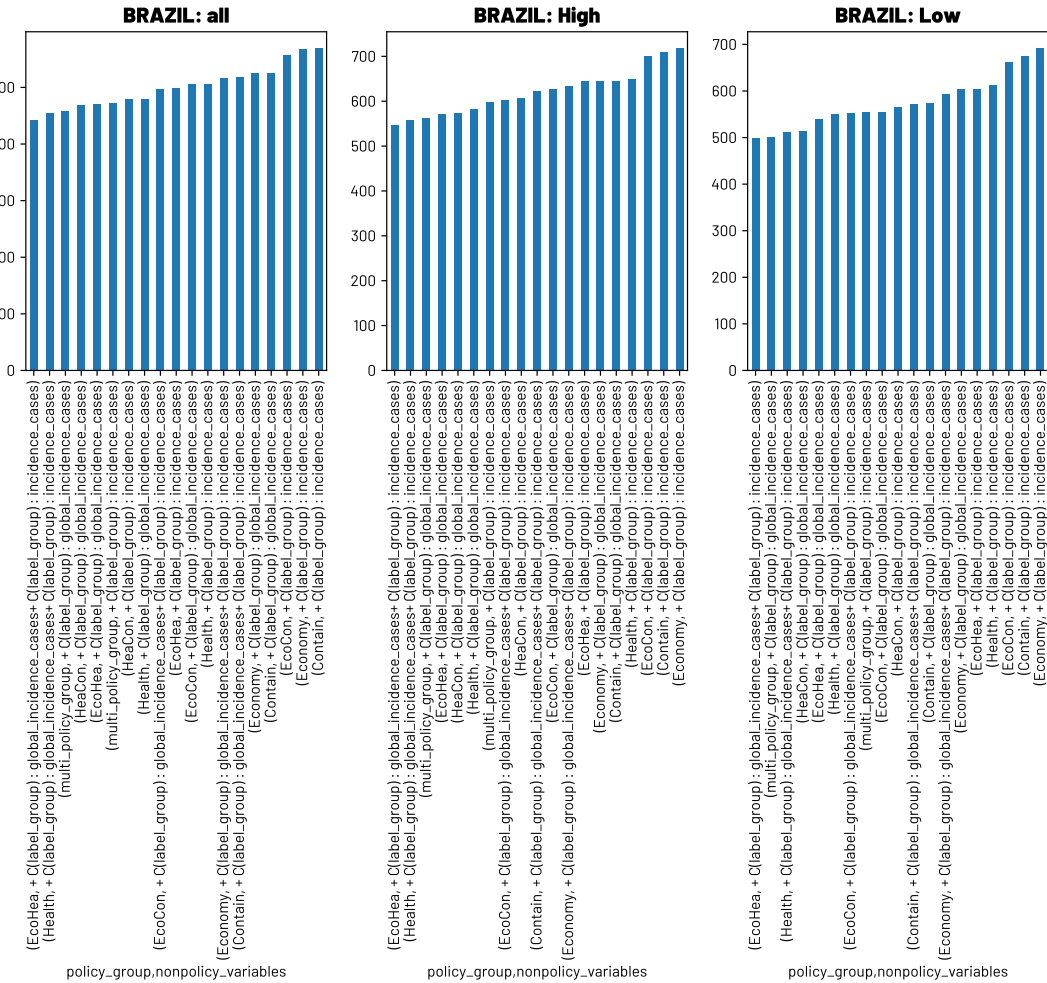


Figure SI 16. *BIC values for all model combinations that do not show any significant multicollinearity. Regression is performed only on Brazil mobility and epidemiological data.*

162 To more precisely understand single policies association with mobility behaviour we would need to
163 disaggregate policy indices into single policy types. However, due to the limited amount of policy activation
164 and loosening over 2020, strong multicollinearity arises by including all single-policy indices without any
165 further selection. To overcome this issue, we focus our attention on Containment policies which are found
166 to be hierarchically the most important policy group in modeling mobility behaviour.

Containment index is thus disaggregated into 5 different single-policy indices which include: school closure, workplace closure, public transport closure, stay-at-home requirements, and internal movement restriction policies.

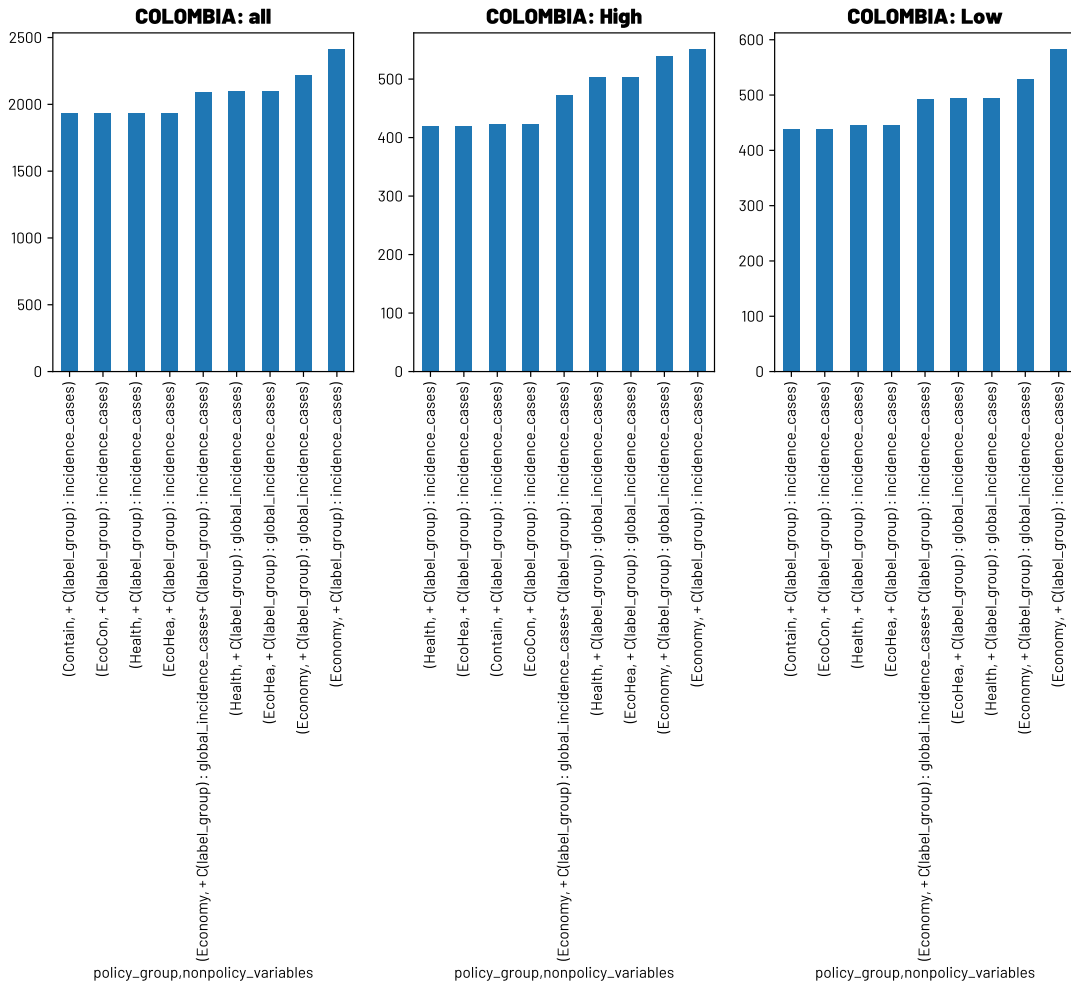


Figure SI 17. *BIC values for all model combinations that do not show any significant multicollinearity.* Regression is performed only on Colombia mobility and epidemiological data.

170

B. Robustness tests for single-policy indices' model

171

In this section we perform multiple modeling robustness tests to check results' reliability. In particular, we are interested in confirming the robustness of the different association levels between low-wealth individuals working in high-wealth neighbourhoods and low-wealth individuals working in low-wealth neighbourhoods. Results reported in the main manuscript shows that all considered policies, with the exception of closures of public transports, do not have a disproportionate association with wealth-specific behavioural response when looking at commuting behaviour.

177

To this end, we structure this section as follow. First, we test that changing the time window over which the regression is performed do not hamper our results, provided that large-enough time span is included to have a minimum amount of policy index changes to be analysed. Second, we test our model including also

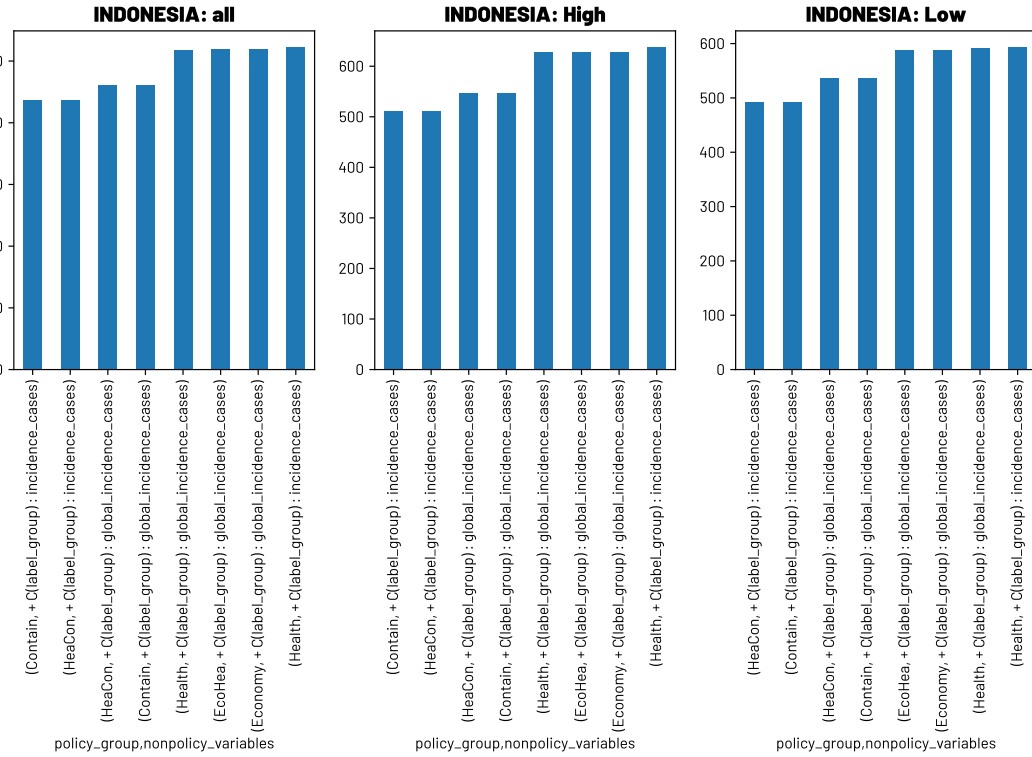


Figure SI 18. *BIC values for all model combinations that do not show any significant multicollinearity.* Regression is performed only on Indonesia mobility and epidemiological data.

180 other variables from different policy group types. Namely, we report parameter estimates for the single-
 181 policy regression including Containment and Economic single-policy indices, as it is the highest ranked
 182 model with more than one policy group. Third, we check results robustness when only one epidemiological
 183 variable is used in the model.

184 The results presented in the main paper are recovered in all robustness tests for which enough statistics
 185 is available. Countries with few changes in specific single-policy indices do not always provide significant
 186 results, but average results values show consistency with the results reported in the main manuscript.

187 *1. Modeling on different periods*

188 We focus our attention on two different periods: the first including only early pandemic period, spanning
 189 from February 11, 2020 to May 10, 2020; the second spanning from February 11, 2020 to the end of the
 190 year.

192 Results shows that including the early period of the pandemic in the regression we recover the results
 193 discussed in the main manuscript, where parameters are estimated starting from April 11, 2020 until the
 194 end of 2020. In particular, including the entire pandemic period during 2020 returns significantly different

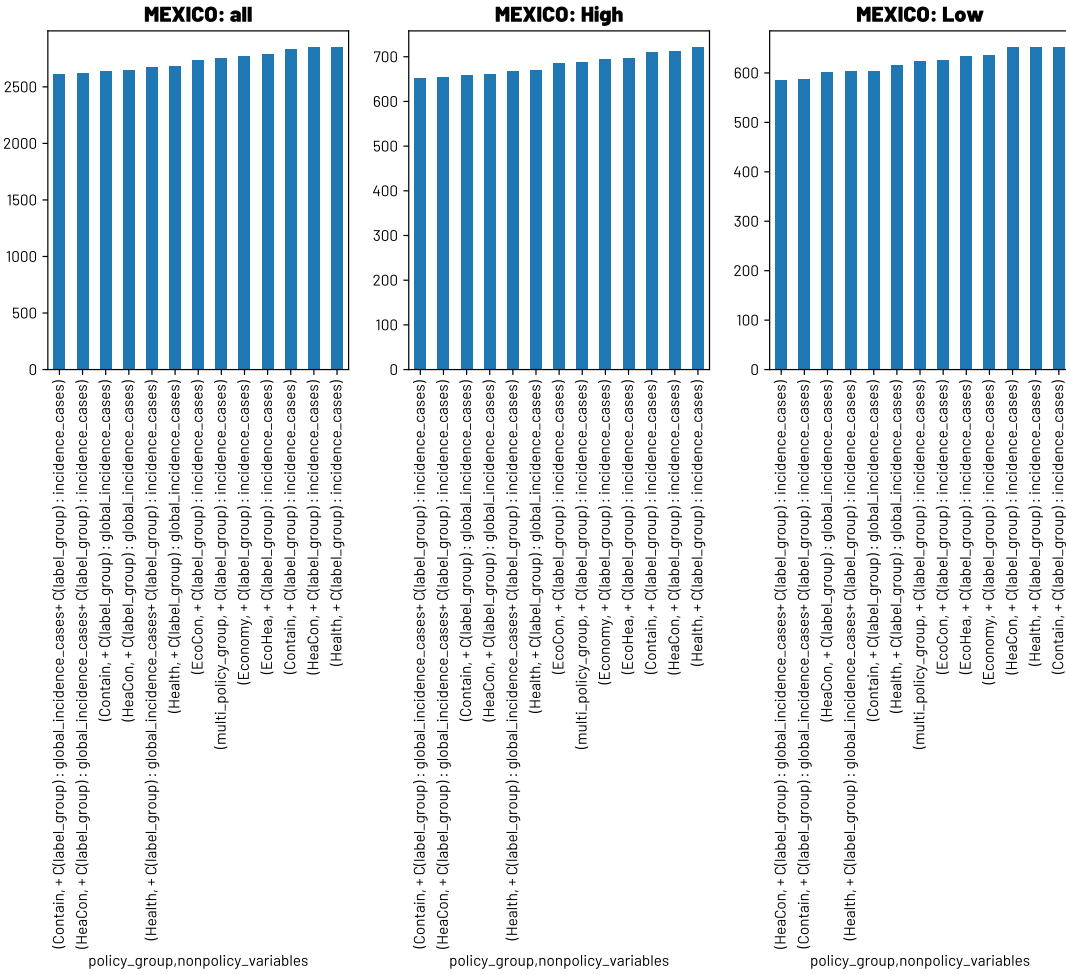


Figure SI 19. *BIC values for all model combinations that do not show any significant multicollinearity. Regression is performed only on Mexico mobility and epidemiological data.*

195 coefficient values for the high-wealth and the low-wealth groups (see Fig. SI 22-left). We stress that the
 196 choice of the time window negatively impact the reliability of the model in the case of the early months of
 197 the pandemic, Fig. SI 22-right. High levels of multicollinearity are found if only those months are included
 198 in the regression. Nevertheless, we always find significant differences in transport closures' values between
 199 high-wealth and low-wealth groups, with high-wealth having greater parameter values.

200

2. Cross-validation on different country sets

201 To further test the robustness of our results, we perform our regression analysis on different subsets of
 202 countries, removing one country at a time.

203 Results show that, while significant differences are not always recovered, the difference in the estimate

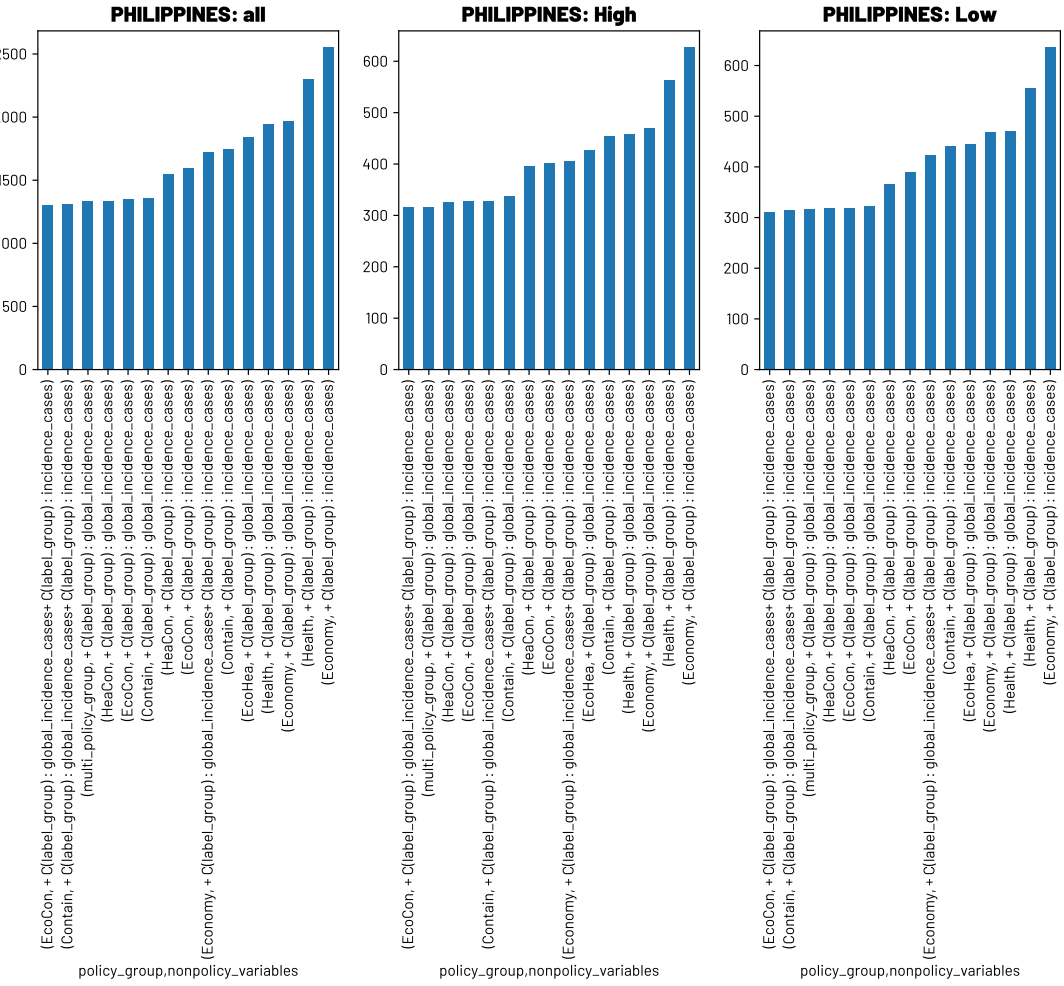


Figure SI 20. *BIC values for all model combinations that do not show any significant multicollinearity.* Regression is performed only on Philippines mobility and epidemiological data.

204 of the parameters is always greater for low-wealth individuals working in high-wealth neighbourhoods. We
 205 stress that also in this case, limiting the regression to a smaller set of countries results in higher levels of
 206 multicollinearity. Nevertheless, all covariates in the models show VIF scores smaller than 4.

207

3. Modeling with additional policy indices

208 We also test our results against the addition of more policy indices. In particular, following the procedure
 209 in Sec. SI 10 A, we select the second best model (in terms of BIC values) including two groups of policy
 210 types: Containment and Economic policies. These two policy groups are divided and each single-policy
 211 index is included in the model. In particular, the economy single-policy indices that are added are i) income
 212 support policies, and ii) debt or contract relief policies (see [8, 12] for more details on the definition of those

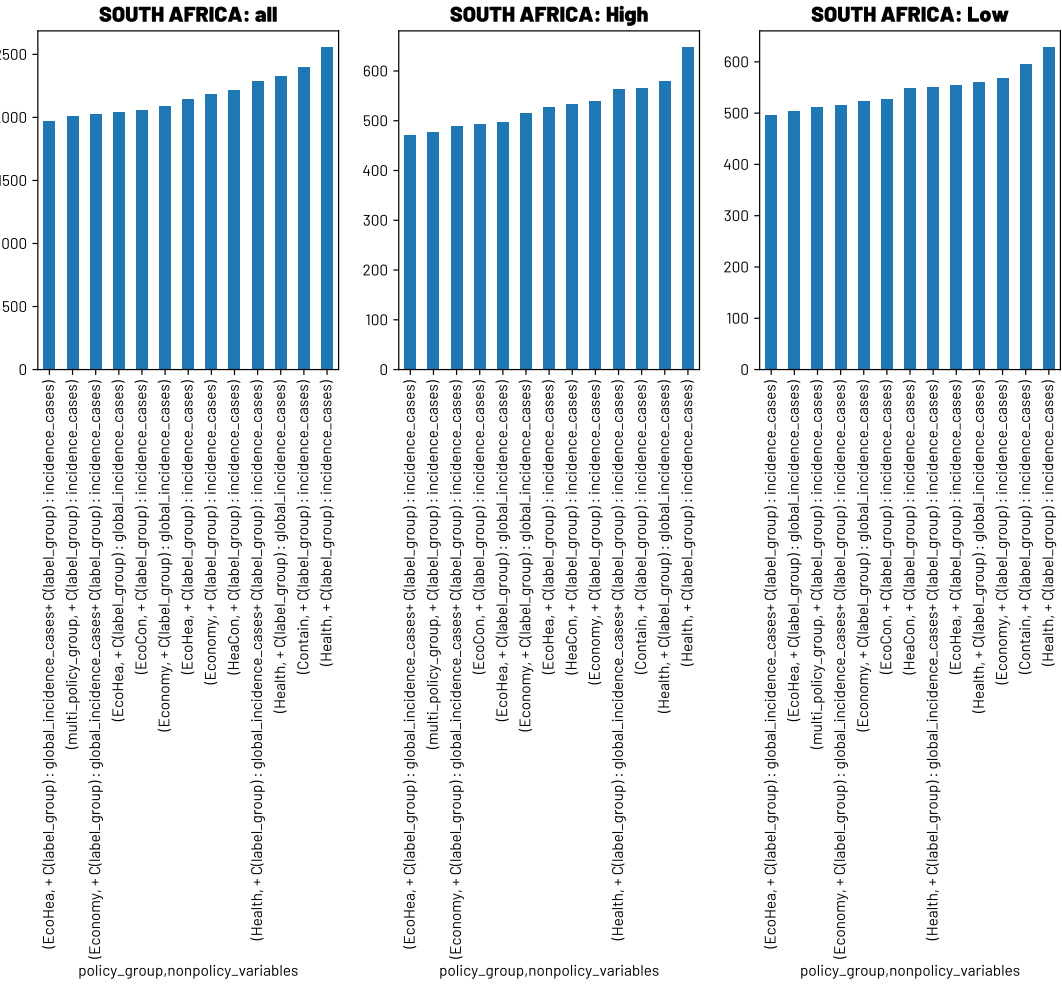


Figure SI 21. *BIC values for all model combinations that do not show any significant multicollinearity.* Regression is performed only on South Africa mobility and epidemiological data.

213 groups). Figure SI 24 shows that both indices are negatively associated with suspension of commuting
 214 patterns. However no significant difference between wealth groups is found. In contrast, public transport
 215 policies are found to be significantly associated with different parameter values depending on the wealth
 216 groups, with low-wealth individuals working in high-wealth neighbourhoods being more strongly associated
 217 than low-wealth individuals working in low-wealth neighbourhoods.

218

4. Incidence of cases: local and global effects on model

219 To further test the robustness of our results, we perform our regression analysis with two different mod-
 220 els: the first one only including the global incidence of cases, while the second one only including the local
 221 (country specific) incidence of cases. In the model discussed in the main manuscript both epidemiological

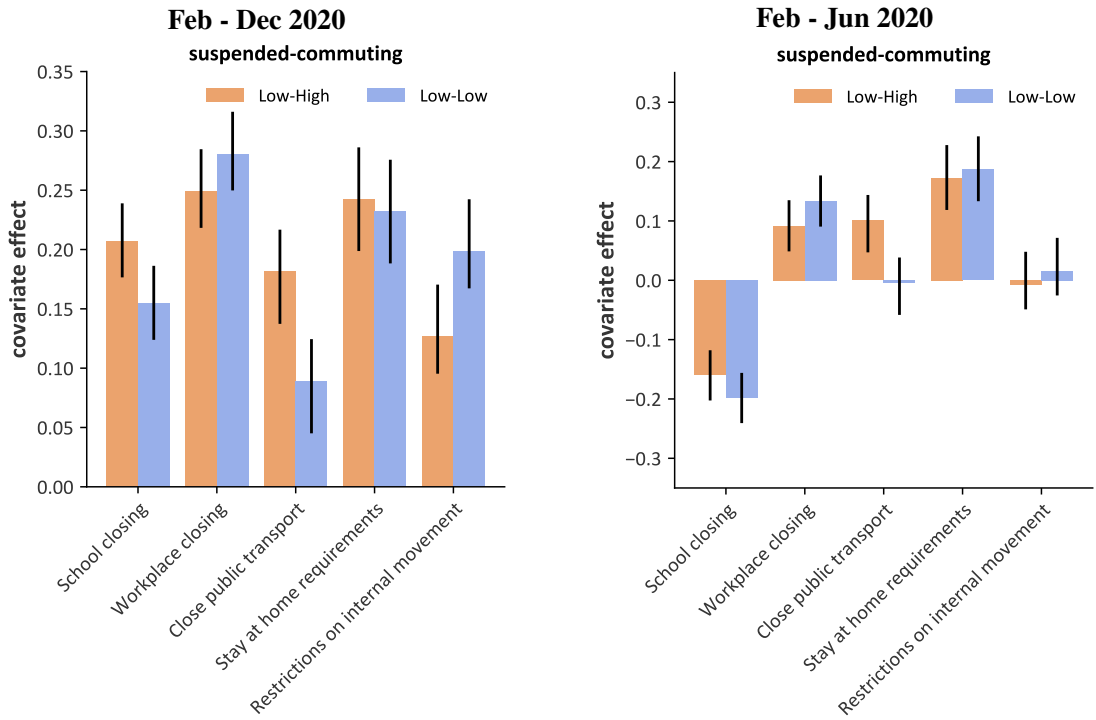


Figure SI 22. *Parameter estimates starting from February 11, 2020 until the end of the year.* Parameters are estimated using the Generalized Least Squares (GLS) method over a period starting from February 11, 2020 until the end of the year. Right: *Parameter estimates for only the early-pandemic period.* Parameters are estimated using GLS method over a period starting from February 11, 2020 until June 10, 2020.

222 indicators where included. Results holds in both cases, as shown in Fig. SI 25-left (for global incidence of
 223 cases only) and in Fig. SI 25-right (for country specific incidence of cases only).

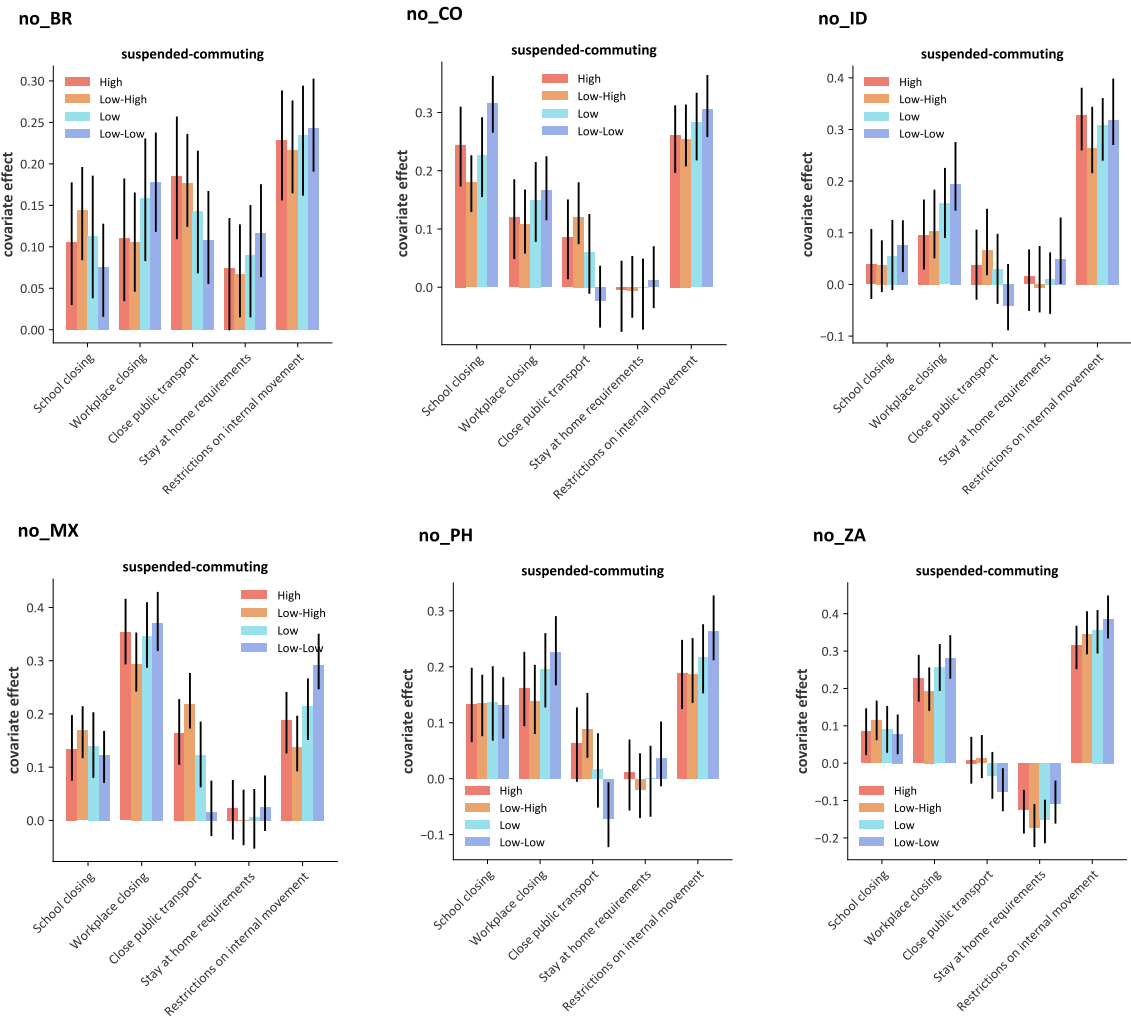


Figure SI 23. *Cross-validating the higher impact of transportation closure on low-wealth individuals working in high wealth neighbourhoods with respect to low-wealth individuals working in low-wealth neighbourhoods.*

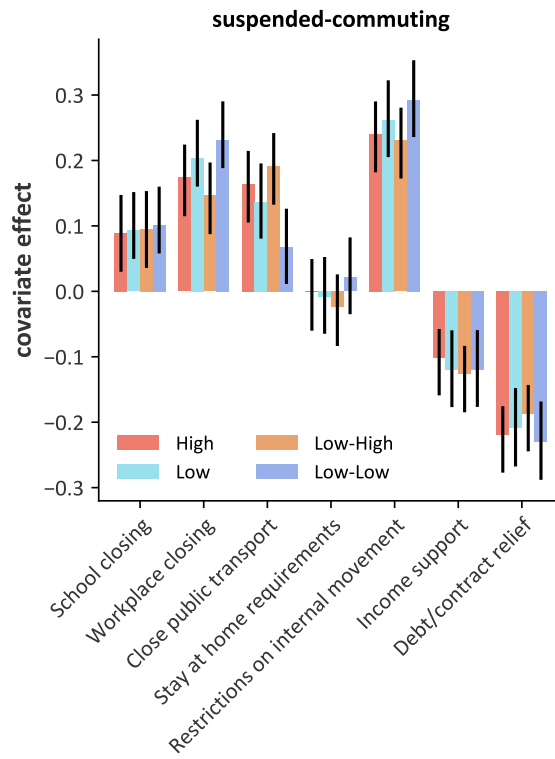


Figure SI 24. *Modeling with additional policy indices.* Results from modeling the fraction of individuals suspending their commuting patterns with two additional policy indices: income support policy index and debt/contract relief policy index.

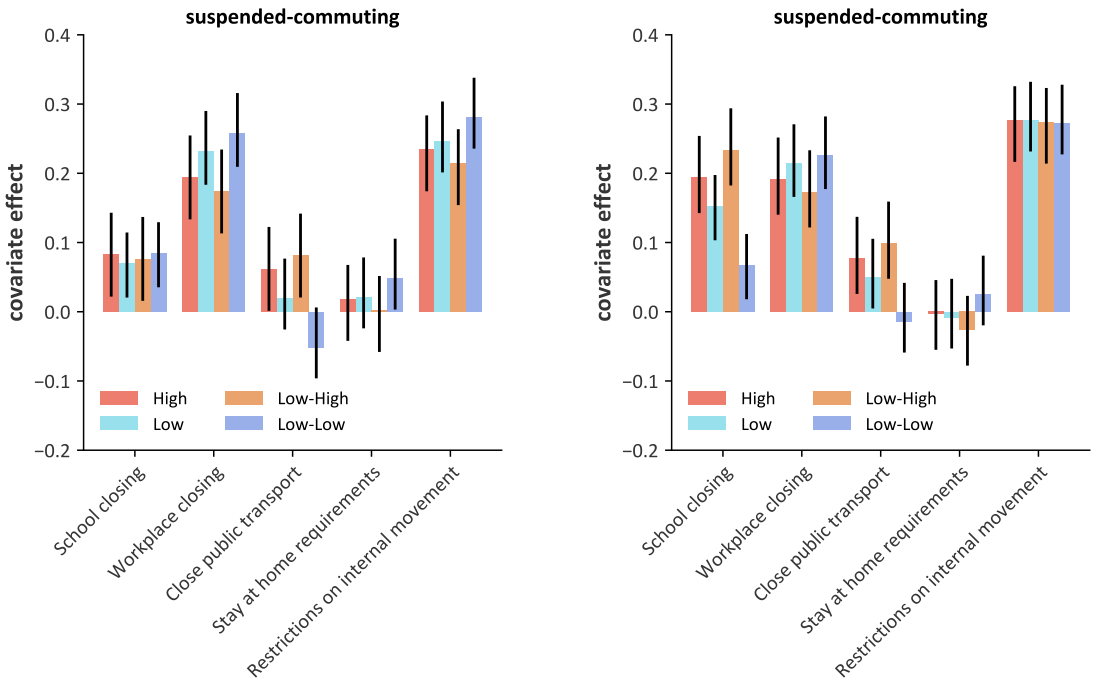


Figure SI 25. *Modeling with only one epidemiological indicator.* Left: parameter values obtained by including as epidemiological indicator only the daily global incidence of cases. Right: parameter values obtained by including as epidemiological indicator only the daily local (for each different country) incidence of cases.

SI 11. MULTI-DIMENSIONAL ANALYSIS OF BEHAVIOURAL RESPONSES

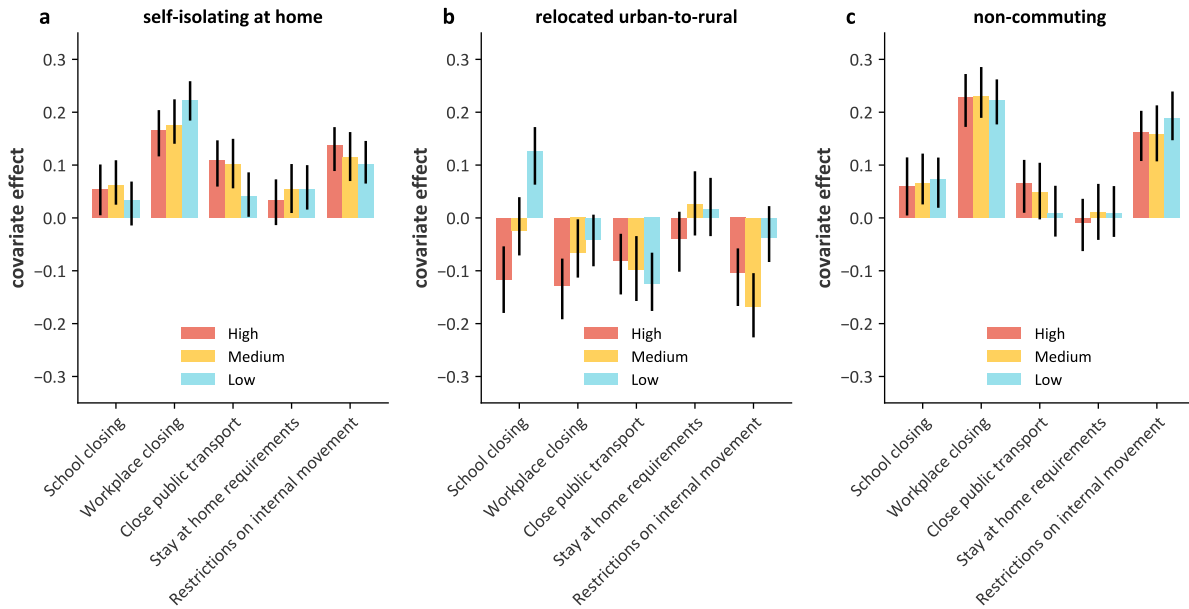


Figure SI 26. Modeling behavioural response to case incidence and containment policies. Panel a-c show the average effect of every policy covariate for the three mobility indicators: self-isolating at home (a), people who stopped commuting (b) and daily migratory flow from urban to rural areas (c).

225 Self-isolating at home, relocating from urban to rural areas, and suspending commuting activities are
 226 important indicators of how deeply an individual changed behaviour over time. We use each of these three
 227 behavioural proxies separately as target variables of a multivariate panel regression model. Each indicator is
 228 studied in terms of both epidemiological conditions and enacted containment policies' covariates. Focusing
 229 on the different enacted policies and their stringency over time we include: school closure, workplace
 230 closure, public transport closure, stay-at-home requirements, and internal movement restriction policies.

231 We find that all the containment policies are positively correlated with an increase in the fraction of
 232 individuals isolating at home as well as with a reduction in the fraction of individuals commuting to their
 233 workplace. In particular, the high-wealth group is associated on average with a higher (significant with
 234 an $\alpha = 0.05$) behavioural recovery to self-isolate when public transport closures are put in place and a
 235 lower propensity with respect to the low-wealth group (see Fig. SI 26a). Self-isolating patterns provide an
 236 important behavioural proxy, e.g., from an epidemiological and social perspective, but they have a limited
 237 power in revealing the potential economic repercussions of containment measures on the job market and in
 238 turn on the economy of a country. With this in mind, we analyse, using the same statistical framework, the
 239 fraction of individuals who suspended their commuting patterns (trips between home and work location)
 240 over time. Thus, we focus only on individuals who were assigned with a work location at least once over

241 the study period. Surprisingly, we find that the significant inter-group differences we found in self-isolation
 242 patterns become less relevant and not statistically significant (see Fig. [SI 26c](#)). Speculatively, this disparities'
 243 reduction can be attributed to an inherently the more similar mobility behaviour of individuals who are
 244 commuting: if we focus only on individuals who are commuting (as long as they are commuting), a part of
 245 their daily mobility behaviour can be explained in terms of commuting patterns, thus limiting behavioural
 246 changes to either the off-commuting pattern or the commuting pattern interruptions dimensions. In this
 247 respect, we focus on the latter dimension, i.e. the external margin of commuting behaviour, as a proxy
 248 for job interruptions to capture macro disparities in the work-related group-behaviour response to policy
 249 implementation.

250 Significant differences are found also in relocating patterns. However, these results are not-robust and
 251 parameters' values and signs change depending on the robustness tests performed. These results were tested
 252 using the same robustness tests as those used for the model of "suspension of commuting patterns". For this
 253 reason, we decided not to discuss in depth these findings.

254

A. Policy indices over time

255 In order to give a sense of how single-policy indices are behaving for each country over the entire
 256 study period, we report here their values. See Fig. [SI 27](#), where we have depicted the following policy
 257 implementations:

- 258 • **C1:** The index records policies closing schools and universities;
- 259 • **C2:** The index records policies closing workplaces;
- 260 • **C5:** The index records policies closing public transport;
- 261 • **C6:** The index records orders to 'shelter-in-place' and to, otherwise, confine at home;
- 262 • **C7:** The index records policy restrictions on internal movement between cities/regions.

263 Policy implementations concerning the cancelling of public events (C3), limiting public gatherings (C4),
 264 and limiting/controlling international travels (C8) are not included in the analysis as they have limited
 265 impact on individual mobility behaviour at the country-scale. In particular, control of international travels
 266 is expected to have relevant impacts on international-scale mobility, however, we do not have records of
 267 international movements in the data used for this analysis.

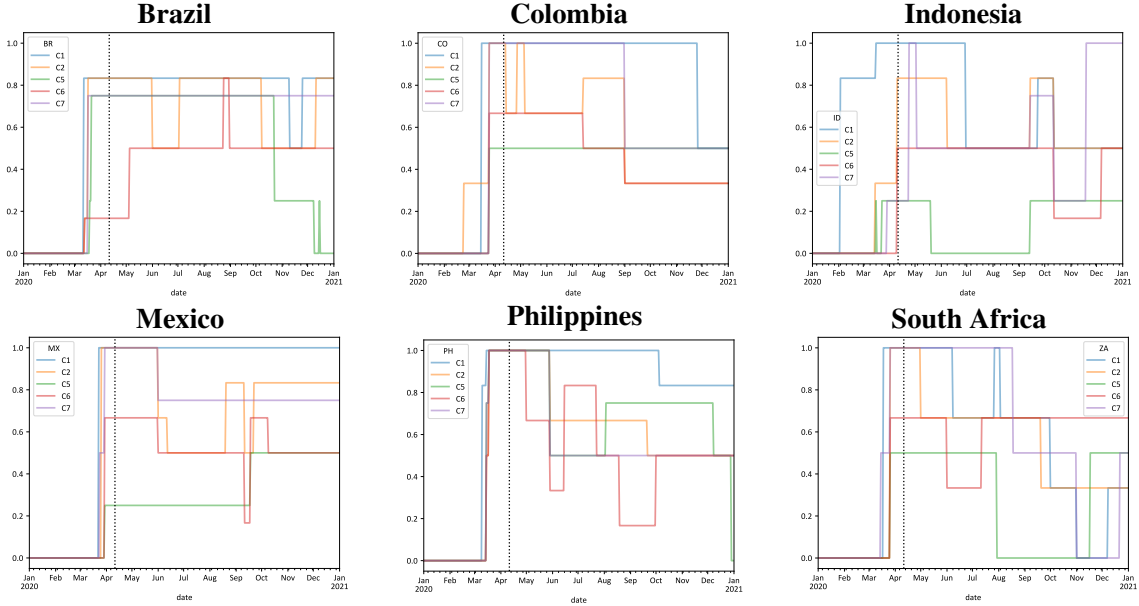


Figure SI 27. *Single-policy indices for containment policy type*. Each panel reports the index values over the entire period of our study. Colours represent the different single-policy indices. The vertical line represents the starting date which we used to perform the regression in the model presented in the main manuscript: April 11, 2020, namely one month after the pandemic declaration.

268 [1] Lauren Alexander, Shan Jiang, Mikel Murga, and Marta C González. Origin–destination trips by purpose and
269 time of day inferred from mobile phone data. *Transportation research part c: emerging technologies*, 58:240–
270 250, 2015.

271 [2] Ulf Aslak and Laura Alessandretti. Infostop: Scalable stop-location detection in multi-user mobility data, 2020.

272 [3] Hugo Barbosa, Fernando B de Lima-Neto, Alexandre Evsukoff, and Ronaldo Menezes. The effect of recency to
273 human mobility. *EPJ Data Science*, 4(1):1–14, 2015.

274 [4] Peter A Burrough, Rachael McDonnell, Rachael A McDonnell, and Christopher D Lloyd. *Principles of geo-*
275 *graphical information systems*. Oxford university press, 2015.

276 [5] Serdar Çolak, Lauren P Alexander, Bernardo G Alvim, Shomik R Mehndiratta, and Marta C González. Ana-
277 lyzing cell phone location data for urban travel: current methods, limitations, and opportunities. *Transportation*
278 *Research Record*, 2526(1):126–135, 2015.

279 [6] Balázs Cs Csáji, Arnaud Browet, Vincent A Traag, Jean-Charles Delvenne, Etienne Huens, Paul Van Dooren,
280 Zbigniew Smoreda, and Vincent D Blondel. Exploring the mobility of mobile phone users. *Physica A: statistical*
281 *mechanics and its applications*, 392(6):1459–1473, 2013.

282 [7] Martin Ester, Hans-Peter Kriegel, Jörg Sander, Xiaowei Xu, et al. A density-based algorithm for discovering
283 clusters in large spatial databases with noise. In *KDD*, volume 96, pages 226–231, 1996.

284 [8] Thomas Hale, Samuel Webster, Petherick Anna, Phillips Toby, and Kira Beatriz. Oxford covid-19 government
285 response tracker. *Blavatnik school of government working paper*, 31:2020–11, 2020.

286 [9] Ramaswamy Hariharan and Kentaro Toyama. Project lachesis: parsing and modeling location histories. In
287 *International Conference on Geographic Information Science*, pages 106–124. Springer, 2004.

288 [10] Luca Pappalardo, Leo Ferres, Manuel Sacasa, Ciro Cattuto, and Loreto Bravo. An individual-level ground truth
289 dataset for home location detection. *arXiv preprint arXiv:2010.08814*, 2010(08814):1–20, 2020.

290 [11] Chaoming Song, Tal Koren, Pu Wang, and Albert-László Barabási. Modelling the scaling properties of human
291 mobility. *Nature physics*, 6(10):818–823, 2010.

292 [12] Oxford COVID-19 Government Response Tracker. Oxcgrt/covid-policy-tracker: Systematic dataset of covid-19
293 policy, from oxford university. Accessed on 2023-02-24.

294 [13] Uber. h3/docs at github master - uber/h3, Accessed on 2020-10-14.

295 [14] Jia Yu, Jinxuan Wu, and Mohamed Sarwat. Geospark: A cluster computing framework for processing large-
296 scale spatial data. In *Proceedings of the 23rd SIGSPATIAL International Conference on Advances in Geographic*
297 *Information Systems*, pages 1–4, 2015.